Supplementary Materials for

Projecting the transmission dynamics of SARS-CoV-2 through the postpandemic period

Stephen M. Kissler*, Christine Tedijanto*, Edward Goldstein, Yonatan H. Grad†‡, Marc Lipsitch†‡

*These authors contributed equally to this work and are co-senior authors.
†These authors contributed equally to this work.
‡Corresponding author. Email: mlipsitc@hsph.harvard.edu (M.L.); ygrad@hsph.harvard.edu (Y.H.G.)

Published 14 April 2020 on *Science* First Release
DOI: 10.1126/science.abb5793

This PDF file includes:

Other Supplementary Material for this manuscript includes the following:
(available at science.sciencemag.org/cgi/content/full/science.abb5793/DC1)

MDAR Reproducibility Checklist (PDF)

Supplement.

Materials and Methods

Data. Viral testing data came from the US National Respiratory and Enteric Virus Surveillance System (NREVSS) (*31*). We extracted the weekly number of total tests for any coronavirus and positive tests for betacoronaviruses HCoV-OC43 and HCoV-HKU1 from all reporting laboratories between 5th July 2014 and 29th June 2019. Dividing the weekly number of positive tests by the total weekly number of tests yielded the weekly percentage of positive tests for each coronavirus.

To estimate the incidence of each betacoronavirus, we used an incidence proxy calculated by multiplying the weekly percentage of positive tests for each coronavirus by the weekly population-weighted proportion of physician visits due to influenza-like illness (ILI) (*32*). The assumptions needed for this proxy to capture true influenza incidence up to a multiplicative constant are described in Goldstein et al. (*32*). Since betacoronaviruses HCoV-OC43 and HCoV-HKU1 are more likely to cause milder cold-like symptoms or acute respiratory infection than ILI, our proxy additionally requires that the proportion of coronavirus cases with ILI is constant over the study period. The weekly proportions of ILI visits were obtained from the US Outpatient Influenza-like Illness Surveillance Network (ILINet) and accessed through the FluView Interactive website (*33*).

Estimating the impact of cross immunity and seasonal drivers of transmission. We used the effective reproduction number, defined as the average number of secondary infections caused by a single infected individual, to quantify the time-varying transmissibility of each coronavirus strain. We estimated the daily effective reproduction number (R_u) based on case counts and the generation interval distribution (*34*), with the following parameterization (*35*):

$$R_u = \sum_{t=u}^{u+i_{max}} \frac{b(t)g(t-u)}{\sum_{a=0}^{i_{max}} b(t-a)g(a)},$$

where $b(t)$ is the strain-level incidence proxy on day t, $g(a)$ is the value of the generation interval distribution at time a, and i_{max} is the maximum generation interval, set as the first day at which over 99% of generation interval distribution had been captured. The generation interval for the four commonly circulating coronaviruses has not been well-studied. In this analysis, we used the estimated serial interval

distribution for SARS (Weibull with mean 8.4 days and standard deviation 3.8 days (*58*)) and varied this assumption in sensitivity analyses based on observations that the serial interval for currently circulating human coronaviruses and SARS-CoV-2 may be considerably lower (*39*, *41*) (**Fig S2**).

To translate the weekly incidence proxies to measures of daily incidence, we followed a previously described spline-based procedure (*36*). For smoothing, the final weekly R is the geometric mean of the daily values in the preceding, current, and following weeks (3-week moving average). We discarded the first three and last three weekly R estimates. To avoid unstable R estimates resulting from periods of low coronavirus activity, we limited our analysis to "in-season" estimates. Seasons were defined as epidemiological week 40 of each year through week 20 of the following year (roughly October through May). Because 2014 consisted of 53 weeks, we truncated the 2014-15 season at week 19 of 2015.

To measure the relative contribution of depletion of susceptibles compared to seasonal forcing in the observed data, we adapted a linear regression model as follows (*36*)**:**

$$log(R_{sij}) = log(R_0 S_0) + \alpha_{sj} + \lambda_s d_{sij} + \delta_s d_{rij} + \sum_{n=1}^{10} \theta_n B_n(i) + \epsilon_{sij}$$

where R_{sij} is the weekly effective reproduction number for strain s in week i of season j, R_0 is the basic reproduction number, S_0 is the fraction of susceptibles at the start of the first season for the reference strain (HCoV-HKU1), and ϵ_{sij} is a normally distributed error term. A dummy variable for each additional strain-season combination (a_{sj}) captures differences in the reproduction number and the starting fraction of susceptibles between strains and over time, but is unable to distinguish between the two. Both R_0 and the fraction of susceptibles may vary by strain and season. If R_0 is assumed to be similar at the start of each season and between the strains, then the dummy variables can be interpreted as differences in immunity. The next two terms estimate the impact of depletion of susceptibles due to infection by the same strain (d_{sij}) and the other betacoronavirus strain (d_{rij}). Depletion of susceptibles for each strain was estimated up to a proportionality constant by the cumulative sum of the incidence proxy over season j through week i. The coefficient on the first term (λ_s) represents the scaling factor between the cumulative incidence proxy and true depletion of susceptibles, while δ_s captures the level of cross-immunity in addition to scaling; both coefficients were allowed to vary by strain. Because specific seasonal drivers (e.g. absolute humidity) of seasonal variation in coronavirus transmission have not been identified, we did not include them in our model but used a cubic basis spline with knots every four weeks to capture fluctuations in seasonal forcing over the year. B_n represents the ten basis functions for a cubic spline with seven internal knots and no intercept, and θ_n the coefficients corresponding to each of these functions.

Dynamic transmission model. We implemented a two-strain ordinary differential equation (ODE) susceptible-exposed-infectious-recovered-susceptible (SEIRS) compartmental model to describe the transmission dynamics of HCoV-OC43 ('strain 1') and HCoV-HKU1 ('strain 2') in the United States. Exposed individuals became infectious at rate ν and infectious individuals recovered at rate γ. Immunity waned at rates σ_1 and σ_2 for HCoV-OC43 and HCoV-HKU1, respectively. The basic reproduction number, R_0, was assumed to be seasonal with a period of 52 weeks, specified by the equation

$$R_0(t) = \max(R_0) * \left[\frac{f}{2} * \cos\left(\frac{2\pi}{52}(t-\phi)\right) + (1-\frac{f}{2})\right]$$

where max(R_0) is the maximum wintertime value of R_0, f is the proportional decline in R_0 that occurs in the summer (f=0 denotes constant R_0 throughout the year), and Φ is the phase shift in weeks. We rounded the length of a year to 52 weeks. The transmission rate $\beta(t)$ is related to the basic reproduction number by the formula (*12*)

$$\beta(t) = \gamma R_0(t).$$

Cross immunity of HCoV-OC43 against HCoV-HKU1 was captured by $\chi_{1,2}$ such that the transmission rate of HCoV-HKU1 to an individual who is exposed to, infected with, or recovered from HCoV-OC43 was reduced by a factor of $1-\chi_{1,2}$, and vice-versa. Individuals died at rate μ such that the average lifespan was $1/\mu$ = 80 years. Fully susceptible individuals were born at the same rate μ to keep the population size constant. A schematic of the model structure is depicted in **Fig S4**.

The entire population was assumed to be susceptible at the start of the simulation period (time = 0). Infection was introduced through a brief, small pulse in the force of infection (an increase of 0.01/week for one half week) for each strain within the first year of the simulation, simulating the establishment of sustained person-to-person transmission. The model was run for 24.5 years to allow the dynamics to reach a steady state, and then the simulated incidence of Strain 1 and Strain 2 were compared with the percent test-positives multiplied by percent of clinic visits for ILI for HCoV-OC43 and HCoV-HKU1, respectively, after scaling the simulated prevalence by a factor ψ. This scaling factor accounts for the difference between % ILI times % positive tests (the units of the data) and the actual prevalence of infection. Model fit was assessed by the SSE between the data and the ψ-scaled simulated prevalence of infection for each strain after taking the logarithm of both. The SSE is proportional to the log likelihood, assuming normal-distributed errors. QQ-plots of the residuals between the data and the model fit support the assumption of normality (**Figure S5**). To determine the parameter values consistent with HCoV-OC43 and HCoV-HKU1 transmission, we used latin hypercube sampling (LHS) (*59*) to simulate transmission for 100,000 combinations of the model parameters sampled uniformly from the ranges

reported in Table 1. We then used the Nelder-Mead algorithm as implemented in *Mathematica's* "NMaximize" function to refine the minimum SSE estimate from the LHS sample. These parameter values are listed in **Table S8**. We were unable to robustly estimate confidence intervals for the estimated parameters because the likelihood surface is jagged due to frequent bifurcations in the model solutions (**Figure S6**). These bifurcations arise due to the competition between strains, which can cause the phase of the outbreaks (*e.g.* whether major HCoV-OC43 outbreaks occur on even or odd years) to shift suddenly as the parameter values change. Instead, we note that the estimated parameter values lie in epidemiologically reasonable ranges, provide a good fit to the incidence data (**Figure 2A**), and provide a good fit to the regression-based effective reproduction number (**Figure 2B-C)**. The effective reproduction number was calculated from the ODE model as the product of the basic reproduction number and the proportion of susceptible individuals in the population at time *t,* accounting for cross-immunity (*60*). For the latin hypercube procedure, the model was implemented in *R* version 3.6.1 (*61*) and integrated using the *lsoda()* function (*62*). The parameter optimization and final model simulations were performed in Mathematica version 12.0.0.0.

Next, we incorporated a third strain into the dynamic transmission model to represent SARS-CoV-2, following the same structure as the model depicted in **Figure S4**. We simulated transmission of HCoV-OC43 and HCoV-HKU1 for 20 years and then simulated the establishment of sustained SARS-CoV-2 transmission using another half-week pulse in the force of infection. We assumed that the latent period for SARS-CoV-2 was 4.6 days (*37–39*) and the infectious period was 5 days, informed by the estimates for the other betacoronaviruses (see **Table S8**). We allowed the cross immunity from SARS-CoV-2 to the other betacoronaviruses and *vice-versa* to range from 0 to 1, the duration of immunity to SARS-CoV-2 to range from 40 weeks to permanent, the seasonal variation in R_0 to vary between none and 40%, and the establishment time to vary throughout 2020. To adjust the amount of seasonal variation in R_0, we held the maximum wintertime value of the sinusoid fixed and adjusted the minimum summertime (baseline) value. This way, smaller degrees of seasonal forcing translated into smaller summertime declines in R_0; for the no-seasonality scenario, R_0 was held fixed at its maximal wintertime value. This choice was informed by observations on the seasonal variation in R_0 for influenza, for which the wintertime R_0 was similar between geographic locations with distinct climates, while the summertime R_0 varied substantially between locations (*12*). For parameter values within these ranges, we measured the annual incidence of infection due to SARS-CoV-2 and the annual SARS-CoV-2 outbreak peak size for the five years following the simulated time of establishment (**Tables S2-7, Figure S7**). We summarized the post-pandemic SARS-CoV-2 dynamics into the categories of annual outbreaks, biennial outbreaks, sporadic outbreaks, or virtual elimination (**Tables S2-7**).

Single-strain transmission model with interventions. To study the qualitative range of social distancing-based interventions that might be effective in curbing SARS-CoV-2 transmission, we implemented an SEIR-type ODE model with a mild illness arm, a hospitalization arm, and a critical care arm. A diagram of the model is given in **Figure S9**, with parameter values in the caption. Since the focus was on the initial pandemic wave, we did not consider waning immunity. We also ignored any cross immunity from the other coronavirus strains against SARS-CoV-2, so that our projections represent a worst-case scenario.

The model depicted in **Figure S9** assumes exponentially-distributed waiting times in each compartment, which may not reflect the true distributions of the latent period, infectious period, or hospital stays. To assess the effect of non-exponential waiting times, we introduced four additional 'dummy' compartments into each internal state of the model (*i.e.* all states except 'susceptible' and 'recovered') so that the waiting times were gamma-distributed (**Figure S17**). The exit rates from each compartment were multiplied by five so that the mean duration in each state remained the same as in the model with exponential waiting times.

Table S1. Estimated regression model coefficients. The intercept represents the natural log of the effective reproduction number (R_0 times fraction susceptible) for HCoV-HKU1 at the start of the 2014-15 season, and each a_{sj} parameter represents the difference in log effective reproduction number for strain s at the start of season j compared to this reference. The λ_s parameters represent the effect of the depletion of susceptibles of strain s (in incidence proxy units) on the effective reproduction number, and the δ_s parameters represent the effect of the depletion of susceptibles of the opposite strain. The θ parameters are the coefficients of the basis spline.

Parameter	Strain (s)	Season (j)	Value
Intercept	HCoV-HKU1	2014-15	0.1278
α_{sj}	HCoV-HKU1	2015-16	-0.1169
α_{sj}	HCoV-HKU1	2016-17	0.0233
α_{sj}	HCoV-HKU1	2017-18	0.0850
α_{sj}	HCoV-HKU1	2018-19	0.0679
α_{sj}	HCoV-OC43	2014-15	-0.0595
α_{sj}	HCoV-OC43	2015-16	-0.1397
α_{sj}	HCoV-OC43	2016-17	-0.0871
α_{sj}	HCoV-OC43	2017-18	-0.0583
α_{sj}	HCoV-OC43	2018-19	-0.0648
λ_s	HCoV-HKU1	-	-0.0025
λ_s	HCoV-OC43	-	-0.0019
δ_s	HCoV-HKU1	-	-0.0013
δ_s	HCoV-OC43	-	-0.0008
θ_1	-	-	0.4509
θ_2	-	-	0.2454
θ_3	-	-	0.4801
θ_4	-	-	0.0705
θ_5	-	-	0.3512
θ_6	-	-	0.0428
θ_7	-	-	0.1494
θ_8	-	-	0.0948
θ_9	-	-	0.2537
θ_{10}	-	-	0.2936

Table S2. Simulated SARS-CoV-2 infections through 2025 with low seasonal forcing. Cumulative projected SARS-CoV-2 cases per 1,000 individuals by year for a representative set of cross immunities, immunity durations, and establishment times. The maximum wintertime R_0 is 2.2 and the summertime R_0 is diminished by a factor of 10% ($R_0 = 2.0$). χ_{3X} represents the degree of cross-immunity induced by infection with SARS-CoV-2 against OC43 and HKU1 and χ_{X3} represents the degree of cross-immunity induced by OC43 or HKU1 infection against SARS-CoV-2. The establishment times correspond to: Winter - week 4 (early February); Spring - week 16 (late April); Summer - week 28 (mid July); Autumn - week 40 (early October). Darker shading corresponds to higher cumulative infection sizes. Years denote epidemiological years, so that 2020 refers to the months between July 2019 and June 2020.

Cross immunity (χ_{3X}, SARS-CoV-2 to HCoV)	Cross immunity (χ_{X3}, HCoV to SARS-CoV-2)	Immunity (wks)	Est. time	2020	2021	2022	2023	2024	2025	Total	Post-pandemic transmission
0.7	0	40	Winter	896	561	600	636	653	658	4004	Annual
0.7	0.3	40	Winter	712	553	609	533	631	563	3602	Annual
0.3	0	40	Winter	896	561	600	636	653	658	4004	Annual
0	0	40	Winter	896	561	600	636	653	658	4004	Annual
0.7	0	104	Winter	853	1	294	195	361	238	1942	Annual
0.7	0.3	104	Winter	673	23	441	34	410	81	1662	Biennial
0.3	0	104	Winter	853	1	291	199	361	237	1941	Annual
0	0	104	Winter	853	1	289	200	361	237	1941	Annual
0.7	0	Permanent	Winter	829	0	0	0	0	0	829	Virtual elimination
0.7	0.3	Permanent	Winter	649	9	0	0	0	0	657	Virtual elimination
0.3	0	Permanent	Winter	829	0	0	0	0	0	829	Virtual elimination
0	0	Permanent	Winter	829	0	0	0	0	0	829	Virtual elimination
0.7	0	40	Spring	604	668	636	638	652	657	3855	Annual
0.7	0.3	40	Spring	229	852	658	543	626	566	3473	Annual
0.3	0	40	Spring	604	668	636	638	652	657	3855	Annual
0	0	40	Spring	604	668	636	638	652	657	3855	Annual
0.7	0	104	Spring	596	229	213	261	346	237	1881	Annual
0.7	0.3	104	Spring	227	478	388	42	392	87	1614	Sporadic
0.3	0	104	Spring	596	229	212	262	346	237	1881	Annual
0	0	104	Spring	596	229	212	262	346	237	1881	Annual
0.7	0	Permanent	Spring	591	207	0	0	0	0	797	Virtual elimination
0.7	0.3	Permanent	Spring	226	433	0	0	0	0	660	Virtual elimination
0.3	0	Permanent	Spring	591	207	0	0	0	0	797	Virtual elimination
0	0	Permanent	Spring	591	207	0	0	0	0	797	Virtual elimination
0.7	0	40	Summer	0	969	746	672	657	657	3702	Annual
0.7	0.3	40	Summer	0	884	688	589	602	584	3347	Annual
0.3	0	40	Summer	0	969	746	672	657	657	3702	Annual
0	0	40	Summer	0	969	746	672	657	657	3702	Annual
0.7	0	104	Summer	0	840	6	479	199	261	1785	Sporadic
0.7	0.3	104	Summer	0	756	68	366	194	307	1691	Sporadic
0.3	0	104	Summer	0	840	5	480	197	263	1784	Sporadic
0	0	104	Summer	0	840	5	480	197	263	1784	Sporadic
0.7	0	Permanent	Summer	0	810	0	0	0	0	810	Virtual elimination
0.7	0.3	Permanent	Summer	0	718	0	0	0	0	718	Virtual elimination
0.3	0	Permanent	Summer	0	810	0	0	0	0	810	Virtual elimination
0	0	Permanent	Summer	0	810	0	0	0	0	810	Virtual elimination
0.7	0	40	Autumn	0	923	651	649	659	660	3543	Annual
0.7	0.3	40	Autumn	0	854	602	571	598	581	3206	Annual
0.3	0	40	Autumn	0	923	651	649	659	660	3543	Annual
0	0	40	Autumn	0	923	651	649	659	660	3543	Annual
0.7	0	104	Autumn	0	866	0	475	31	406	1777	Biennial
0.7	0.3	104	Autumn	0	791	1	358	210	206	1566	Sporadic
0.3	0	104	Autumn	0	866	0	474	31	405	1777	Biennial
0	0	104	Autumn	0	866	0	474	31	405	1777	Biennial
0.7	0	Permanent	Autumn	0	840	0	0	0	0	840	Virtual elimination
0.7	0.3	Permanent	Autumn	0	761	0	0	0	0	761	Virtual elimination
0.3	0	Permanent	Autumn	0	840	0	0	0	0	840	Virtual elimination
0	0	Permanent	Autumn	0	840	0	0	0	0	840	Virtual elimination

Table S3. Simulated SARS-CoV-2 infections through 2025 with moderate seasonal forcing. Cumulative projected SARS-CoV-2 cases per 1,000 individuals by year for a representative set of cross immunities, immunity durations, and establishment times. The maximum wintertime R_0 is 2.2 and the summertime R_0 is diminished by a factor of 20% ($R_0 = 1.8$). χ_{3X} represents the degree of cross-immunity induced by infection with SARS-CoV-2 against OC43 and HKU1 and χ_{X3} represents the degree of cross-immunity induced by OC43 or HKU1 infection against SARS-CoV-2. The establishment times correspond to: Winter - week 4 (early February); Spring - week 16 (late April); Summer - week 28 (mid July); Autumn - week 40 (early October). Darker shading corresponds to higher cumulative infection sizes. Years denote epidemiological years, so that 2020 refers to the months between July 2019 and June 2020.

Cross immunity (χ3X, SARS-CoV-2 to HCoV)	Cross immunity (χX3, HCoV to SARS-CoV-2)	Immunity (wks)	Est. time	2020	2021	2022	2023	2024	2025	Total	Post-pandemic transmission
0.7	0	40	Winter	873	531	585	612	619	619	3839	Annual
0.7	0.3	40	Winter	654	545	584	485	602	480	3350	Annual
0.3	0	40	Winter	873	531	585	612	619	619	3839	Annual
0	0	40	Winter	873	531	585	612	619	619	3839	Annual
0.7	0	104	Winter	833	1	82	437	269	214	1836	Sporadic
0.7	0.3	104	Winter	620	31	451	4	358	100	1564	Sporadic
0.3	0	104	Winter	833	1	78	442	266	218	1837	Annual
0	0	104	Winter	833	1	77	443	265	219	1837	Annual
0.7	0	Permanent	Winter	810	0	0	0	0	0	810	Virtual elimination
0.7	0.3	Permanent	Winter	599	9	0	0	0	0	608	Virtual elimination
0.3	0	Permanent	Winter	810	0	0	0	0	0	810	Virtual elimination
0	0	Permanent	Winter	810	0	0	0	0	0	810	Virtual elimination
0.7	0	40	Spring	459	741	617	623	624	622	3685	Annual
0.7	0.3	40	Spring	148	851	622	516	596	483	3215	Annual
0.3	0	40	Spring	459	741	617	623	624	622	3685	Annual
0	0	40	Spring	459	741	617	623	624	622	3685	Annual
0.7	0	104	Spring	454	310	332	142	348	162	1748	Annual
0.7	0.3	104	Spring	147	537	325	45	387	38	1479	Biennial
0.3	0	104	Spring	454	310	332	142	348	162	1748	Annual
0	0	104	Spring	454	310	332	142	348	162	1748	Annual
0.7	0	Permanent	Spring	451	280	0	0	0	0	730	Virtual elimination
0.7	0.3	Permanent	Spring	146	447	0	0	0	0	593	Virtual elimination
0.3	0	Permanent	Spring	451	280	0	0	0	0	730	Virtual elimination
0	0	Permanent	Spring	451	280	0	0	0	0	730	Virtual elimination
0.7	0	40	Summer	0	944	688	642	631	625	3530	Annual
0.7	0.3	40	Summer	0	862	621	541	592	485	3101	Annual
0.3	0	40	Summer	0	944	688	642	631	625	3530	Annual
0	0	40	Summer	0	944	688	642	631	625	3530	Annual
0.7	0	104	Summer	0	812	4	506	10	473	1805	Biennial
0.7	0.3	104	Summer	0	742	13	433	23	385	1595	Biennial
0.3	0	104	Summer	0	812	4	506	10	473	1805	Biennial
0	0	104	Summer	0	812	4	506	10	473	1805	Biennial
0.7	0	Permanent	Summer	0	776	0	0	0	0	776	Virtual elimination
0.7	0.3	Permanent	Summer	0	697	0	0	0	0	697	Virtual elimination
0.3	0	Permanent	Summer	0	776	0	0	0	0	776	Virtual elimination
0	0	Permanent	Summer	0	776	0	0	0	0	776	Virtual elimination
0.7	0	40	Autumn	0	918	643	612	613	616	3403	Annual
0.7	0.3	40	Autumn	0	847	541	582	472	611	3053	Annual
0.3	0	40	Autumn	0	918	643	612	613	616	3403	Annual
0	0	40	Autumn	0	918	643	612	613	616	3403	Annual
0.7	0	104	Autumn	0	862	0	305	217	343	1727	Annual
0.7	0.3	104	Autumn	0	787	0	100	438	57	1382	Sporadic
0.3	0	104	Autumn	0	862	0	285	241	338	1725	Annual
0	0	104	Autumn	0	862	0	284	241	338	1725	Annual
0.7	0	Permanent	Autumn	0	835	0	0	0	0	835	Virtual elimination
0.7	0.3	Permanent	Autumn	0	757	0	0	0	0	757	Virtual elimination
0.3	0	Permanent	Autumn	0	835	0	0	0	0	835	Virtual elimination
0	0	Permanent	Autumn	0	835	0	0	0	0	835	Virtual elimination

Table S4. Simulated SARS-CoV-2 infections through 2025 with high seasonal forcing. Cumulative projected SARS-CoV-2 cases per 1,000 individuals by year for a representative set of cross immunities, immunity durations, and establishment times. The maximum wintertime R_0 is 2.2 and the summertime R_0 is diminished by a factor of 40% (R_0 = 1.3). χ_{3X} represents the degree of cross-immunity induced by infection with SARS-CoV-2 against OC43 and HKU1 and χ_{X3} represents the degree of cross-immunity induced by OC43 or HKU1 infection against SARS-CoV-2. The establishment times correspond to: Winter - week 4 (early February); Spring - week 16 (late April); Summer - week 28 (mid July); Autumn - week 40 (early October). Darker shading corresponds to higher cumulative infection sizes. Years denote epidemiological years, so that 2020 refers to the months between July 2019 and June 2020.

Cross immunity (χ_{3X}, SARS-CoV-2 to HCoV)	Cross immunity (χ_{X3}, HCoV to SARS-CoV-2)	Immunity (wks)	Est. time	2020	2021	2022	2023	2024	2025	Total	Post-pandemic transmission
0.7	0	40	Winter	818	367	624	549	539	545	3442	Annual
0.7	0.3	40	Winter	515	555	307	608	157	678	2820	Biennial
0.3	0	40	Winter	818	367	624	549	539	545	3442	Annual
0	0	40	Winter	818	367	624	549	539	545	3442	Annual
0.7	0	104	Winter	784	0	1	601	0	6	1393	Sporadic
0.7	0.3	104	Winter	493	68	324	20	258	189	1352	Sporadic
0.3	0	104	Winter	784	0	1	600	0	5	1390	Sporadic
0	0	104	Winter	784	0	1	600	0	5	1390	Sporadic
0.7	0	Permanent	Winter	764	0	0	0	0	0	764	Virtual elimination
0.7	0.3	Permanent	Winter	479	7	0	0	0	0	487	Virtual elimination
0.3	0	Permanent	Winter	764	0	0	0	0	0	764	Virtual elimination
0	0	Permanent	Winter	764	0	0	0	0	0	764	Virtual elimination
0.7	0	40	Spring	192	856	614	512	557	539	3270	Annual
0.7	0.3	40	Spring	57	821	338	605	162	666	2650	Biennial
0.3	0	40	Spring	192	856	614	512	557	539	3270	Annual
0	0	40	Spring	192	856	614	512	557	539	3270	Annual
0.7	0	104	Spring	191	582	12	512	0	72	1370	Biennial
0.7	0.3	104	Spring	57	695	0	2	452	4	1211	Sporadic
0.3	0	104	Spring	191	582	12	512	0	71	1369	Biennial
0	0	104	Spring	191	582	12	512	0	71	1369	Biennial
0.7	0	Permanent	Spring	191	415	0	0	0	0	606	Virtual elimination
0.7	0.3	Permanent	Spring	57	618	0	0	0	0	675	Virtual elimination
0.3	0	Permanent	Spring	191	415	0	0	0	0	606	Virtual elimination
0	0	Permanent	Spring	191	415	0	0	0	0	606	Virtual elimination
0.7	0	40	Summer	0	912	645	497	565	538	3157	Annual
0.7	0.3	40	Summer	0	845	293	630	158	668	2594	Biennial
0.3	0	40	Summer	0	912	645	497	565	538	3157	Annual
0	0	40	Summer	0	912	645	497	565	538	3157	Annual
0.7	0	104	Summer	0	803	0	119	504	0	1426	Sporadic
0.7	0.3	104	Summer	0	760	0	0	259	327	1346	Sporadic
0.3	0	104	Summer	0	803	0	122	501	1	1426	Sporadic
0	0	104	Summer	0	803	0	122	501	1	1426	Sporadic
0.7	0	Permanent	Summer	0	753	0	0	0	0	753	Virtual elimination
0.7	0.3	Permanent	Summer	0	714	0	0	0	0	714	Virtual elimination
0.3	0	Permanent	Summer	0	753	0	0	0	0	753	Virtual elimination
0	0	Permanent	Summer	0	753	0	0	0	0	753	Virtual elimination
0.7	0	40	Autumn	0	912	529	554	542	542	3078	Annual
0.7	0.3	40	Autumn	0	835	165	692	167	666	2525	Biennial
0.3	0	40	Autumn	0	912	529	554	542	542	3078	Annual
0	0	40	Autumn	0	912	529	554	542	542	3078	Annual
0.7	0	104	Autumn	0	856	0	0	856	0	0	Sporadic
0.7	0.3	104	Autumn	0	779	0	0	41	604	1424	Sporadic
0.3	0	104	Autumn	0	856	0	0	573	1	1430	Sporadic
0	0	104	Autumn	0	856	0	0	573	1	1430	Sporadic
0.7	0	Permanent	Autumn	0	828	0	0	0	0	828	Virtual elimination
0.7	0.3	Permanent	Autumn	0	749	0	0	0	0	749	Virtual elimination
0.3	0	Permanent	Autumn	0	828	0	0	0	0	828	Virtual elimination
0	0	Permanent	Autumn	0	828	0	0	0	0	828	Virtual elimination

Table S5. Peak SARS-CoV-2 prevalence through 2025 with low seasonal forcing. Peak simulated SARS-CoV-2 cases per 1,000 individuals by year for a representative set of cross immunities, immunity durations, and establishment times. The maximum wintertime R_0 is 2.2 and the summertime R_0 is diminished by a factor of 10% (R_0 = 2.0). χ_{3X} represents the degree of cross-immunity induced by infection with SARS-CoV-2 against OC43 and HKU1 and χ_{X3} represents the degree of cross-immunity induced by OC43 or HKU1 infection against SARS-CoV-2. The establishment times correspond to: Winter - week 4 (early February); Spring - week 16 (late April); Summer - week 28 (mid July); Autumn - week 40 (early October). Darker shading corresponds to higher cumulative infection sizes. Years denote epidemiological years, so that 2020 refers to the months between July 2019 and June 2020.

Cross immunity (χ3X, SARS-CoV-2 to HCoV)	Cross immunity (χX3, HCoV to SARS-CoV-2)	Immunity (wks)	Est. time	2020	2021	2022	2023	2024	2025	Max	Post-pandemic transmission
0.7	0	40	Winter	95.6	29.1	20.7	19.0	17.6	16.8	95.6	Annual
0.7	0.3	40	Winter	49.7	21.4	18.6	14.2	17.4	16.6	49.7	Annual
0.3	0	40	Winter	95.6	29.1	20.7	19.0	17.6	16.8	95.6	Annual
0	0	40	Winter	95.6	29.1	20.7	19.0	17.6	16.8	95.6	Annual
0.7	0	104	Winter	94.3	0.2	21.0	18.3	10.0	8.4	94.3	Annual
0.7	0.3	104	Winter	48.4	3.8	18.7	1.2	14.0	2.3	48.4	Biennial
0.3	0	104	Winter	94.3	0.2	21.0	18.6	10.1	8.4	94.3	Annual
0	0	104	Winter	94.3	0.2	21.0	18.7	10.1	8.4	94.3	Annual
0.7	0	Permanent	Winter	93.4	0.1	0.0	0.0	0.0	0.0	93.4	Virtual elimination
0.7	0.3	Permanent	Winter	47.6	2.8	0.0	0.0	0.0	0.0	47.6	Virtual elimination
0.3	0	Permanent	Winter	93.4	0.1	0.0	0.0	0.0	0.0	93.4	Virtual elimination
0	0	Permanent	Winter	93.4	0.1	0.0	0.0	0.0	0.0	93.4	Virtual elimination
0.7	0	40	Spring	83.2	73.3	14.8	17.0	17.2	16.8	83.2	Annual
0.7	0.3	40	Spring	38.6	46.6	12.7	12.8	17.0	16.8	46.6	Annual
0.3	0	40	Spring	83.2	73.3	14.8	17.0	17.2	16.8	83.2	Annual
0	0	40	Spring	83.2	73.3	14.8	17.0	17.2	16.8	83.2	Annual
0.7	0	104	Spring	81.8	71.0	16.8	16.7	9.3	8.0	81.8	Annual
0.7	0.3	104	Spring	38.1	45.2	17.0	1.3	13.7	2.5	45.2	Sporadic
0.3	0	104	Spring	81.8	71.0	16.8	16.7	9.3	8.0	81.8	Annual
0	0	104	Spring	81.8	71.0	16.8	16.7	9.4	8.0	81.8	Annual
0.7	0	Permanent	Spring	81.0	69.5	0.0	0.0	0.0	0.0	81.0	Virtual elimination
0.7	0.3	Permanent	Spring	37.8	44.4	0.0	0.0	0.0	0.0	44.4	Virtual elimination
0.3	0	Permanent	Spring	81.0	69.5	0.0	0.0	0.0	0.0	81.0	Virtual elimination
0	0	Permanent	Spring	81.0	69.5	0.0	0.0	0.0	0.0	81.0	Virtual elimination
0.7	0	40	Summer	0.0	84.0	18.4	13.6	15.8	16.4	84.0	Annual
0.7	0.3	40	Summer	0.0	56.9	18.4	15.1	17.5	18.2	56.9	Annual
0.3	0	40	Summer	0.0	84.0	18.4	13.6	15.8	16.4	84.0	Annual
0	0	40	Summer	0.0	84.0	18.4	13.6	15.8	16.4	84.0	Annual
0.7	0	104	Summer	0.0	82.5	0.7	21.6	10.3	9.6	82.5	Sporadic
0.7	0.3	104	Summer	0.0	55.3	5.8	7.4	5.1	9.0	55.3	Sporadic
0.3	0	104	Summer	0.0	82.5	0.7	21.7	10.2	9.7	82.5	Sporadic
0	0	104	Summer	0.0	82.5	0.7	21.7	10.2	9.7	82.5	Sporadic
0.7	0	Permanent	Summer	0.0	81.5	0.0	0.0	0.0	0.0	81.5	Virtual elimination
0.7	0.3	Permanent	Summer	0.0	54.3	0.0	0.0	0.0	0.0	54.3	Virtual elimination
0.3	0	Permanent	Summer	0.0	81.5	0.0	0.0	0.0	0.0	81.5	Virtual elimination
0	0	Permanent	Summer	0.0	81.5	0.0	0.0	0.0	0.0	81.5	Virtual elimination
0.7	0	40	Autumn	0.0	95.8	31.3	20.9	17.5	16.5	95.8	Annual
0.7	0.3	40	Autumn	0.0	71.4	28.5	21.2	20.2	18.9	71.4	Annual
0.3	0	40	Autumn	0.0	95.8	31.3	20.9	17.5	16.5	95.8	Annual
0	0	40	Autumn	0.0	95.8	31.3	20.9	17.5	16.5	95.8	Annual
0.7	0	104	Autumn	0.0	94.3	0.0	28.5	1.6	12.8	94.3	Biennial
0.7	0.3	104	Autumn	0.0	69.9	0.1	13.8	6.6	5.3	69.9	Sporadic
0.3	0	104	Autumn	0.0	94.3	0.0	28.6	1.6	12.8	94.3	Biennial
0	0	104	Autumn	0.0	94.3	0.0	28.6	1.6	12.8	94.3	Biennial
0.7	0	Permanent	Autumn	0.0	93.4	0.0	0.0	0.0	0.0	93.4	Virtual elimination
0.7	0.3	Permanent	Autumn	0.0	68.9	0.0	0.0	0.0	0.0	68.9	Virtual elimination
0.3	0	Permanent	Autumn	0.0	93.4	0.0	0.0	0.0	0.0	93.4	Virtual elimination
0	0	Permanent	Autumn	0.0	93.4	0.0	0.0	0.0	0.0	93.4	Virtual elimination

Table S6. Peak SARS-CoV-2 prevalence through 2025 with moderate seasonal forcing. Peak simulated SARS-CoV-2 cases per 1,000 individuals by year for a representative set of cross immunities, immunity durations, and establishment times. The maximum wintertime R_0 is 2.2 and the summertime R_0 is diminished by a factor of 20% (R_0 = 1.8). χ_{3X} represents the degree of cross-immunity induced by infection with SARS-CoV-2 against OC43 and HKU1 and χ_{X3} represents the degree of cross-immunity induced by OC43 or HKU1 infection against SARS-CoV-2. The establishment times correspond to: Winter - week 4 (early February); Spring - week 16 (late April); Summer - week 28 (mid July); Autumn - week 40 (early October). Darker shading corresponds to higher cumulative infection sizes. Years denote epidemiological years, so that 2020 refers to the months between July 2019 and June 2020.

Cross immunity (χ3X, SARS-CoV-2 to HCoV)	Cross immunity (χX3, HCoV to SARS-CoV-2)	Immunity (wks)	Est. time	2020	2021	2022	2023	2024	2025	Max	Post-pandemic transmission
0.7	0	40	Winter	91.5	30.3	26.6	29.9	31.2	31.5	91.5	Annual
0.7	0.3	40	Winter	44.2	24.2	26.9	19.0	27.4	19.3	44.2	Annual
0.3	0	40	Winter	91.5	30.3	26.6	29.9	31.2	31.5	91.5	Annual
0	0	40	Winter	91.5	30.3	26.6	29.9	31.2	31.5	91.5	Annual
0.7	0	104	Winter	90.2	0.2	9.2	13.2	11.3	6.5	90.2	Sporadic
0.7	0.3	104	Winter	43.1	3.8	20.8	0.2	17.8	4.0	43.1	Sporadic
0.3	0	104	Winter	90.2	0.2	8.8	13.3	11.2	6.6	90.2	Annual
0	0	104	Winter	90.2	0.2	8.7	13.3	11.2	6.6	90.2	Annual
0.7	0	Permanent	Winter	89.4	0.1	0.0	0.0	0.0	0.0	89.4	Virtual elimination
0.7	0.3	Permanent	Winter	42.4	2.9	0.0	0.0	0.0	0.0	42.4	Virtual elimination
0.3	0	Permanent	Winter	89.4	0.1	0.0	0.0	0.0	0.0	89.4	Virtual elimination
0	0	Permanent	Winter	89.4	0.1	0.0	0.0	0.0	0.0	89.4	Virtual elimination
0.7	0	40	Spring	65.0	64.1	22.1	28.9	30.9	31.5	65.0	Annual
0.7	0.3	40	Spring	22.4	31.2	22.1	20.7	28.3	20.0	31.2	Annual
0.3	0	40	Spring	65.0	64.1	22.1	28.9	30.9	31.5	65.0	Annual
0	0	40	Spring	65.0	64.1	22.1	28.9	30.9	31.5	65.0	Annual
0.7	0	104	Spring	63.8	62.5	17.1	4.3	10.1	6.7	63.8	Annual
0.7	0.3	104	Spring	22.2	30.0	14.7	1.4	16.0	1.3	30.0	Biennial
0.3	0	104	Spring	63.8	62.5	17.1	4.3	10.1	6.7	63.8	Annual
0	0	104	Spring	63.8	62.5	17.1	4.3	10.1	6.7	63.8	Annual
0.7	0	Permanent	Spring	63.0	61.5	0.0	0.0	0.0	0.0	63.0	Virtual elimination
0.7	0.3	Permanent	Spring	22.0	29.3	0.0	0.0	0.0	0.0	29.3	Virtual elimination
0.3	0	Permanent	Spring	63.0	61.5	0.0	0.0	0.0	0.0	63.0	Virtual elimination
0	0	Permanent	Spring	63.0	61.5	0.0	0.0	0.0	0.0	63.0	Virtual elimination
0.7	0	40	Summer	0.0	69.1	22.7	27.4	30.3	31.3	69.1	Annual
0.7	0.3	40	Summer	0.0	47.6	27.3	25.1	30.0	20.4	47.6	Annual
0.3	0	40	Summer	0.0	69.1	22.7	27.4	30.3	31.3	69.1	Annual
0	0	40	Summer	0.0	69.1	22.7	27.4	30.3	31.3	69.1	Annual
0.7	0	104	Summer	0.0	67.5	0.4	26.3	0.7	21.8	67.5	Biennial
0.7	0.3	104	Summer	0.0	45.8	0.7	19.5	0.8	16.5	45.8	Biennial
0.3	0	104	Summer	0.0	67.5	0.4	26.3	0.7	21.8	67.5	Biennial
0	0	104	Summer	0.0	67.5	0.4	26.3	0.7	21.8	67.5	Biennial
0.7	0	Permanent	Summer	0.0	66.5	0.0	0.0	0.0	0.0	66.5	Virtual elimination
0.7	0.3	Permanent	Summer	0.0	44.6	0.0	0.0	0.0	0.0	44.6	Virtual elimination
0.3	0	Permanent	Summer	0.0	66.5	0.0	0.0	0.0	0.0	66.5	Virtual elimination
0	0	Permanent	Summer	0.0	66.5	0.0	0.0	0.0	0.0	66.5	Virtual elimination
0.7	0	40	Autumn	0.0	92.4	40.0	33.2	31.8	31.6	92.4	Annual
0.7	0.3	40	Autumn	0.0	69.2	30.0	30.4	19.7	28.5	69.2	Annual
0.3	0	40	Autumn	0.0	92.4	40.0	33.2	31.8	31.6	92.4	Annual
0	0	40	Autumn	0.0	92.4	40.0	33.2	31.8	31.6	92.4	Annual
0.7	0	104	Autumn	0.0	90.9	0.0	20.2	15.0	11.9	90.9	Annual
0.7	0.3	104	Autumn	0.0	67.6	0.0	6.7	9.4	1.6	67.6	Sporadic
0.3	0	104	Autumn	0.0	90.9	0.0	19.7	16.3	12.0	90.9	Annual
0	0	104	Autumn	0.0	90.9	0.0	19.7	16.3	12.0	90.9	Annual
0.7	0	Permanent	Autumn	0.0	89.9	0.0	0.0	0.0	0.0	89.9	Virtual elimination
0.7	0.3	Permanent	Autumn	0.0	66.6	0.0	0.0	0.0	0.0	66.6	Virtual elimination
0.3	0	Permanent	Autumn	0.0	89.9	0.0	0.0	0.0	0.0	89.9	Virtual elimination
0	0	Permanent	Autumn	0.0	89.9	0.0	0.0	0.0	0.0	89.9	Virtual elimination

Table S7. Peak SARS-CoV-2 prevalence through 2025 with high seasonal forcing. Peak simulated SARS-CoV-2 cases per 1,000 individuals by year for a representative set of cross immunities, immunity durations, and establishment times. The maximum wintertime R_0 is 2.2 and the summertime R_0 is diminished by a factor of 40% (R_0 = 1.3). χ_{3X} represents the degree of cross-immunity induced by infection with SARS-CoV-2 against OC43 and HKU1 and χ_{X3} represents the degree of cross-immunity induced by OC43 or HKU1 infection against SARS-CoV-2. The establishment times correspond to: Winter - week 4 (early February); Spring - week 16 (late April); Summer - week 28 (mid July); Autumn - week 40 (early October). Darker shading corresponds to higher cumulative infection sizes. Years denote epidemiological years, so that 2020 refers to the months between July 2019 and June 2020.

Cross immunity (χ3X, SARS-CoV-2 to HCoV)	Cross immunity (χX3, HCoV to SARS-CoV-2)	Immunity (wks)	Est. time	2020	2021	2022	2023	2024	2025	Max	Post-pandemic transmission
0.7	0	40	Winter	82.9	21.8	35.9	38.1	35.7	36.4	82.9	Annual
0.7	0.3	40	Winter	33.7	33.3	14.5	38.9	7.1	40.3	40.3	Biennial
0.3	0	40	Winter	82.9	21.8	35.9	38.1	35.7	36.4	82.9	Annual
0	0	40	Winter	82.9	21.8	35.9	38.1	35.7	36.4	82.9	Annual
0.7	0	104	Winter	81.7	0.2	0.1	48.1	0.0	0.4	81.7	Sporadic
0.7	0.3	104	Winter	33.0	2.8	14.1	0.9	12.2	9.2	33.0	Sporadic
0.3	0	104	Winter	81.7	0.2	0.1	48.2	0.0	0.4	81.7	Sporadic
0	0	104	Winter	81.7	0.2	0.0	48.2	0.0	0.4	81.7	Sporadic
0.7	0	Permanent	Winter	80.9	0.1	0.0	0.0	0.0	0.0	80.9	Virtual elimination
0.7	0.3	Permanent	Winter	32.6	2.3	0.0	0.0	0.0	0.0	32.6	Virtual elimination
0.3	0	Permanent	Winter	80.9	0.1	0.0	0.0	0.0	0.0	80.9	Virtual elimination
0	0	Permanent	Winter	80.9	0.1	0.0	0.0	0.0	0.0	80.9	Virtual elimination
0.7	0	40	Spring	24.9	26.0	44.1	34.1	36.6	36.3	44.1	Annual
0.7	0.3	40	Spring	5.4	36.1	16.8	38.2	7.4	39.4	39.4	Biennial
0.3	0	40	Spring	24.9	26.0	44.1	34.1	36.6	36.3	44.1	Annual
0	0	40	Spring	24.9	26.0	44.1	34.1	36.6	36.3	44.1	Annual
0.7	0	104	Spring	24.6	25.4	0.5	34.7	0.1	4.6	34.7	Biennial
0.7	0.3	104	Spring	5.4	30.8	0.0	0.1	29.4	0.4	30.8	Sporadic
0.3	0	104	Spring	24.6	25.4	0.5	34.7	0.1	4.5	34.7	Biennial
0	0	104	Spring	24.6	25.4	0.5	34.7	0.1	4.5	34.7	Biennial
0.7	0	Permanent	Spring	24.3	25.0	0.0	0.0	0.0	0.0	25.0	Virtual elimination
0.7	0.3	Permanent	Spring	5.3	27.0	0.0	0.0	0.0	0.0	27.0	Virtual elimination
0.3	0	Permanent	Spring	24.3	25.0	0.0	0.0	0.0	0.0	25.0	Virtual elimination
0	0	Permanent	Spring	24.3	25.0	0.0	0.0	0.0	0.0	25.0	Virtual elimination
0.7	0	40	Summer	0.0	52.7	48.5	32.9	36.7	36.3	52.7	Annual
0.7	0.3	40	Summer	0.0	49.0	14.4	38.2	7.3	39.1	49.0	Biennial
0.3	0	40	Summer	0.0	52.7	48.5	32.9	36.7	36.3	52.7	Annual
0	0	40	Summer	0.0	52.7	48.5	32.9	36.7	36.3	52.7	Annual
0.7	0	104	Summer	0.0	50.0	0.0	7.5	21.1	0.1	50.0	Sporadic
0.7	0.3	104	Summer	0.0	46.0	0.0	0.0	13.8	16.4	46.0	Sporadic
0.3	0	104	Summer	0.0	50.0	0.0	7.7	21.0	0.1	50.0	Sporadic
0	0	104	Summer	0.0	50.0	0.0	7.7	21.0	0.1	50.0	Sporadic
0.7	0	Permanent	Summer	0.0	48.4	0.0	0.0	0.0	0.0	48.4	Virtual elimination
0.7	0.3	Permanent	Summer	0.0	44.1	0.0	0.0	0.0	0.0	44.1	Virtual elimination
0.3	0	Permanent	Summer	0.0	48.4	0.0	0.0	0.0	0.0	48.4	Virtual elimination
0	0	Permanent	Summer	0.0	48.4	0.0	0.0	0.0	0.0	48.4	Virtual elimination
0.7	0	40	Autumn	0.0	87.1	37.0	35.7	36.6	36.1	87.1	Annual
0.7	0.3	40	Autumn	0.0	66.2	8.0	39.1	7.8	38.7	66.2	Biennial
0.3	0	40	Autumn	0.0	87.1	37.0	35.7	36.6	36.1	87.1	Annual
0	0	40	Autumn	0.0	87.1	37.0	35.7	36.6	36.1	87.1	Annual
0.7	0	104	Autumn	0.0	85.4	0.0	0.0	0.0	0.0	85.4	Sporadic
0.7	0.3	104	Autumn	0.0	64.5	0.0	0.0	2.1	37.1	64.5	Sporadic
0.3	0	104	Autumn	0.0	85.4	0.0	0.0	46.6	0.2	85.4	Sporadic
0	0	104	Autumn	0.0	85.4	0.0	0.0	46.6	0.2	85.4	Sporadic
0.7	0	Permanent	Autumn	0.0	84.3	0.0	0.0	0.0	0.0	84.3	Virtual elimination
0.7	0.3	Permanent	Autumn	0.0	63.3	0.0	0.0	0.0	0.0	63.3	Virtual elimination
0.3	0	Permanent	Autumn	0.0	84.3	0.0	0.0	0.0	0.0	84.3	Virtual elimination
0	0	Permanent	Autumn	0.0	84.3	0.0	0.0	0.0	0.0	84.3	Virtual elimination

Table S8. Parameter values for the two-strain SEIRS transmission model.

Parameter	Range for LHS	Interpretation	Units	Estimated value
f	[0, 0.6]	Fractional summertime decline in R_0	none	0.21
max(R_0)	[1, 3]	Maximal wintertime R_0	none	2.2
ϕ	[-8, 8]	Seasonal R_0 shift	weeks	2.0
$1/\sigma_1$	[25, 100]	Waning immunity period, strain 1	weeks	45
$1/\sigma_2$	[25, 100]	Waning immunity period, strain 2	weeks	45
χ_{12}	[0, 1]	Cross immunity, strain 1 against strain 2	none	0.78
χ_{21}	[0, 1]	Cross immunity, strain 2 against strain 1	none	0.51
$1/\nu$	[3, 14]	Latent period	days	3.0
$1/\gamma$	[3, 14]	Infectious period	days	5.0
ψ	[0.01, 0.1]	Conversion from prevalence to % positive multiplied by % ILI	none	0.06
$1/\mu$	80 (fixed)	Average lifespan	years	80

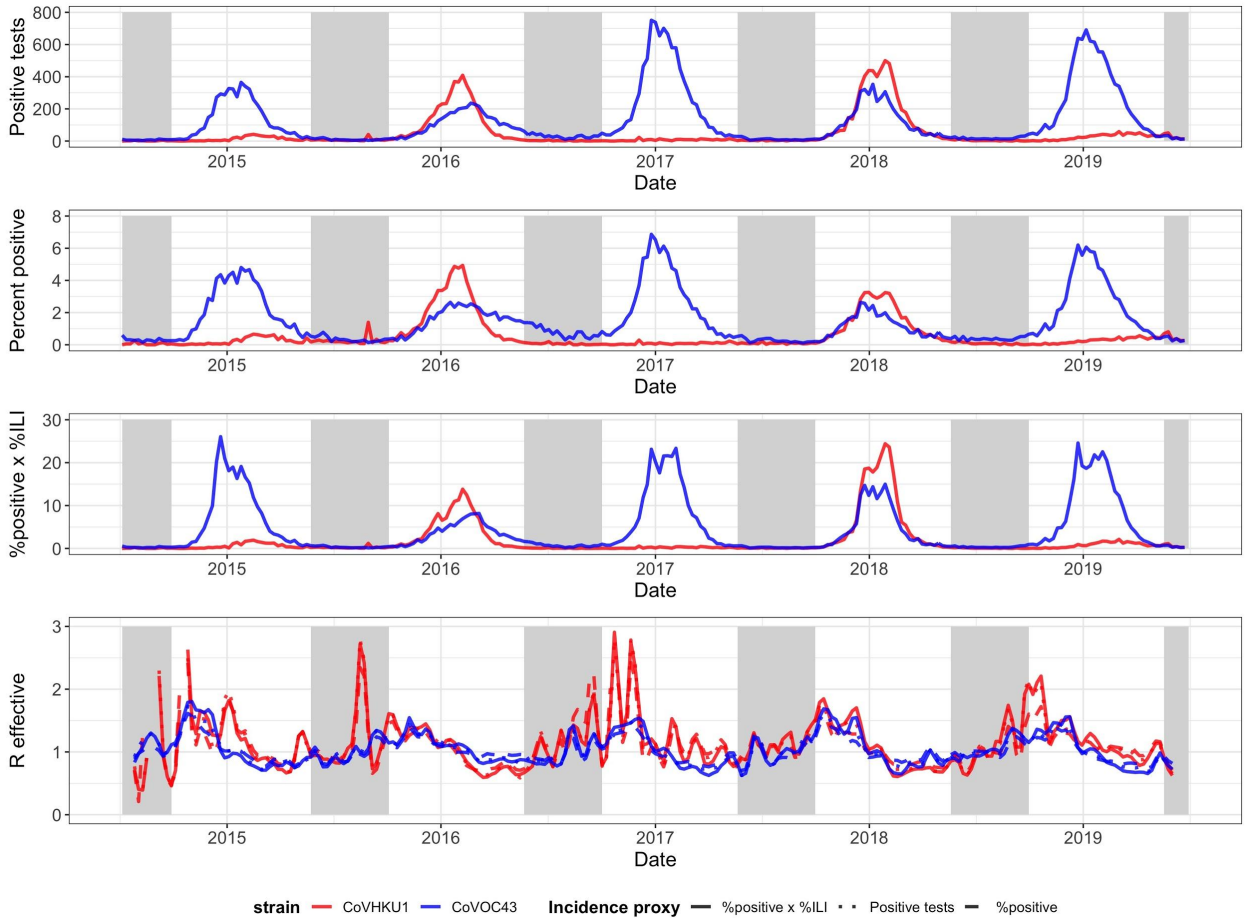

Figure S1. Incidence proxies and effective reproduction numbers by strain. HCoV-HKU1 shown in red and HCoV-OC43 shown in blue. (A) Weekly number of positive tests from NREVSS. (B) Weekly percent positive laboratory tests. (C) Weekly percent positive laboratory tests multiplied by percent of clinic visits for ILI. (D) Comparison of effective reproduction numbers by incidence measure using SARS serial interval. Twelve estimates for HCoV-HKU1 that were greater than 3 (all occurring at the end of 2014) are not shown.

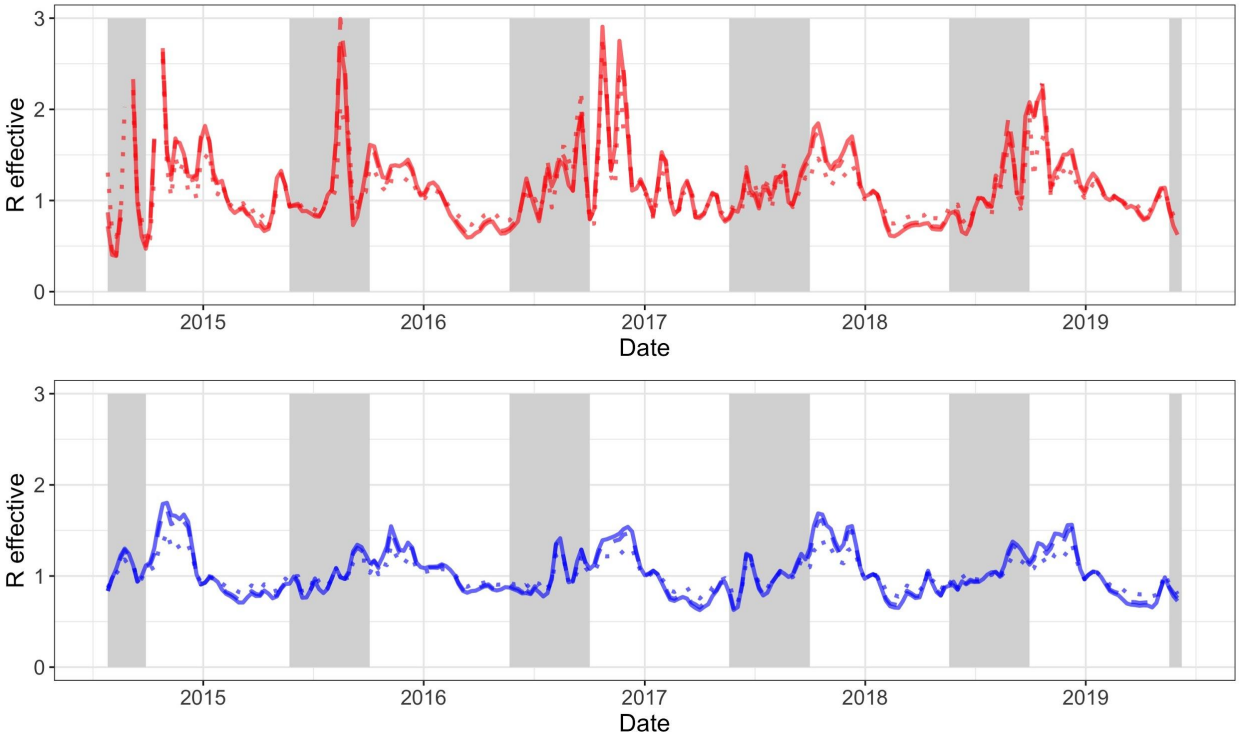

Figure S2. Estimates of weekly effective reproduction numbers under different assumptions for the serial interval. HCoV-HKU1 shown in top panel and HCoV-OC43 shown in bottom panel. Serial interval distributions were defined as follows - SARS (solid): Weibull distribution with mean of 8.4 days and s.d. of 3.8 days (shape=2.35, scale=9.48); Li *et al*. 2020 (*41*) (dashed): Gamma distribution with mean of 7.5 days and s.d. of 3.4 days (shape=4.87, scale=1.54); Linton *et al*. 2020 (*39*) (dotted): Weibull distribution with mean of 4.8 days and s.d. of 2.3 days (shape=2.20, scale=5.42). Sections shaded in gray are out-of-season (epidemiological weeks 21-39). Three estimates for HCoV-HKU1 that were greater than 3 (all occurring at the end of 2014) are not shown.

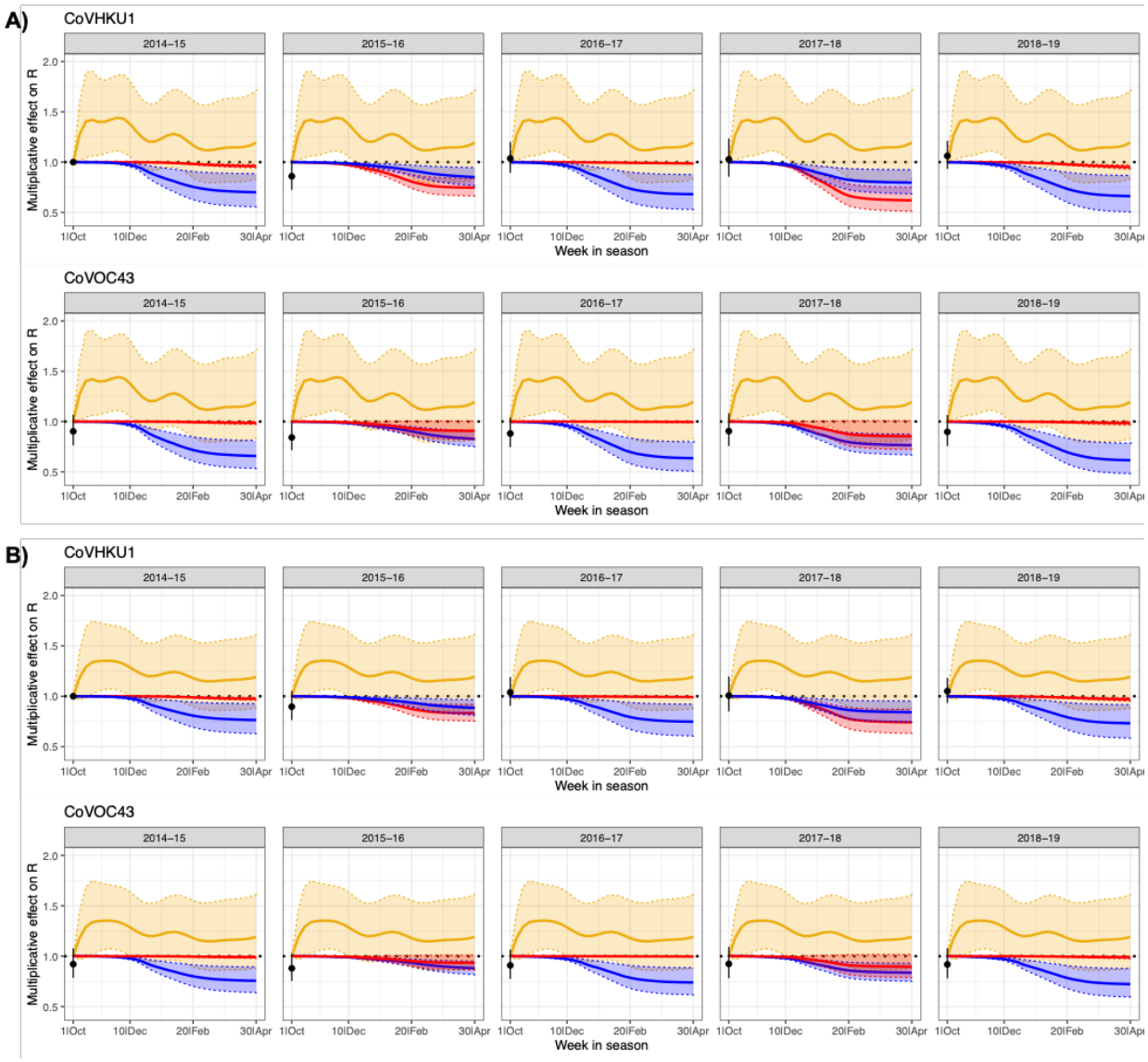

Figure S3. Effects of depletion of susceptibles and seasonality on the effective reproduction number under different assumptions for the serial interval. Estimated multiplicative effects of HCoV-HKU1 incidence (red), HCoV-OC43 incidence (blue), and seasonal forcing (gold) on weekly effective reproduction numbers of HCoV-HKU1 (top) and HCoV-OC43 (bottom), with 95% confidence intervals. Effective reproduction numbers were estimated using serial intervals estimated in (A) Li *et al*. 2020 (*41*) and (B) Linton *et al*. 2020 (*39*). The black dot (with 95% confidence interval) plotted at the start of each season is the estimated coefficient for that strain and season compared to the 2014-15 HCoV-HKU1 season. The seasonal forcing spline is set to 1 at the first week of the season (no intercept). On the x-axis, the first "week in season" corresponds to epidemiological week 40.

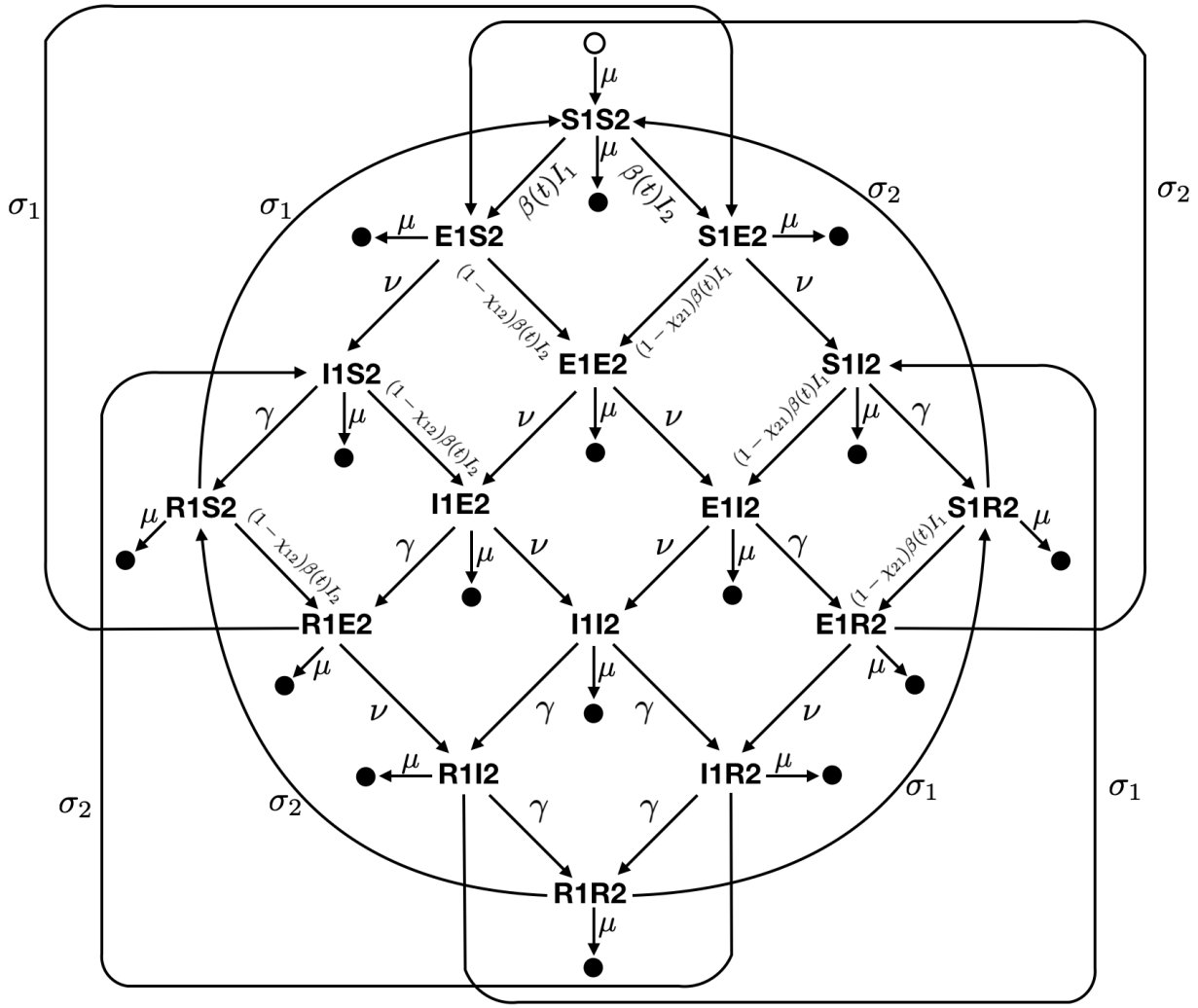

Figure S4. Schematic diagram of the two-strain SEIRS transmission model. Diagram of the two-strain compartmental SEIRS model used to describe the transmission of HCoV-OC43 and HCoV-HKU1 in the United States. Epidemiological compartments are represented by the bold letter-number pairs, such that an individual in compartment S1S2 is susceptible to both strains, while a person in compartment I1E2 is infectious with strain 1 and has been exposed to strain 2. Filled circles represent death and the open circle represents births. Transition rates are given next to the arrows between compartments. Estimated parameter values are listed in **Table S8**.

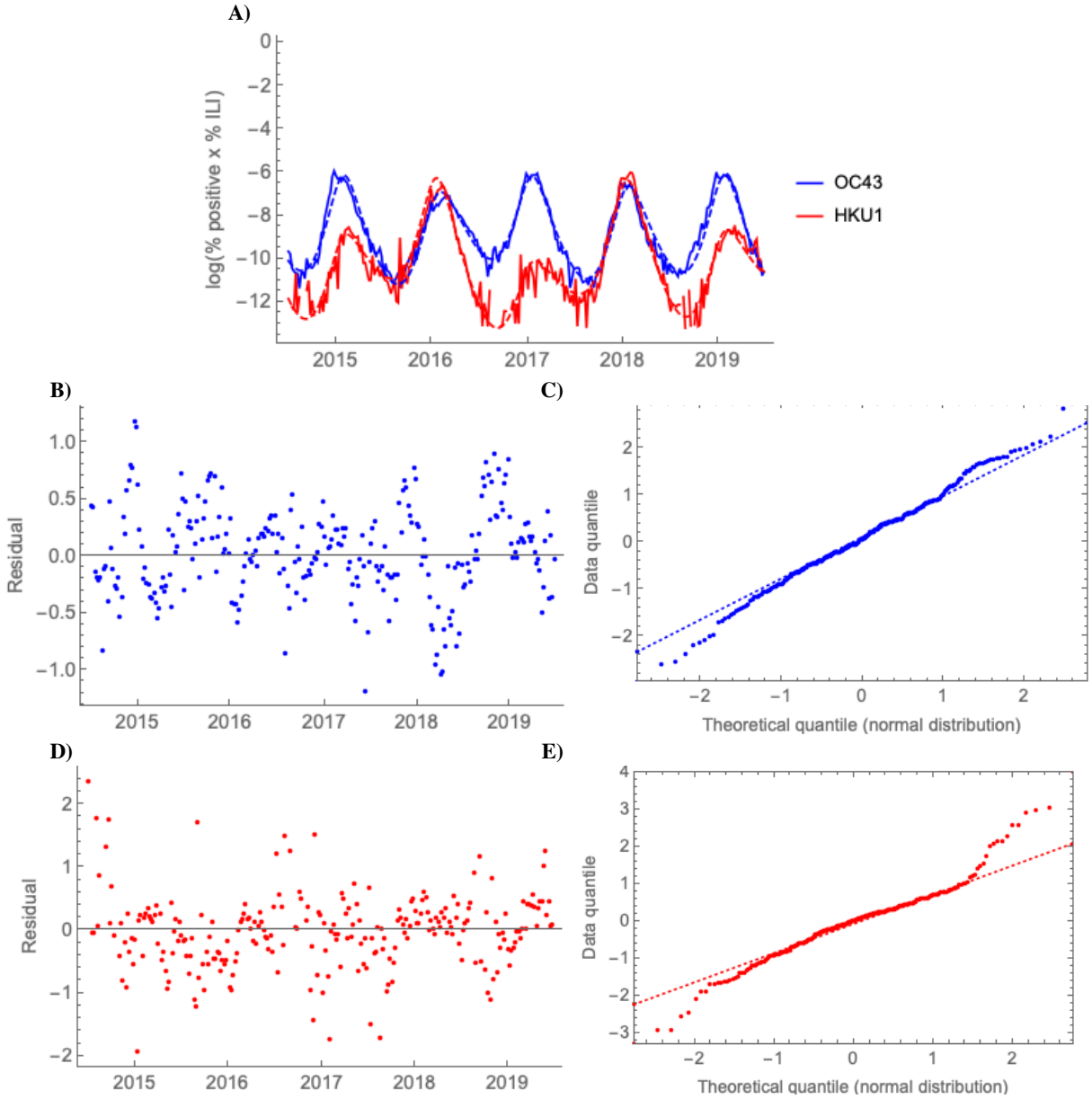

Figure S5. Model fit and residuals on a log scale. A) Logarithm of the NREVSS HCoV-OC43 (blue, solid) and HCoV-HKU1 (red, solid) data and logarithm of the simulated prevalence of HCoV-OC43 (blue, dashed) and HCoV-HKU1 (red, dashed) infection. B) Residual errors from the HCoV-OC43 fit on the log scale. C) Q-Q plot of the quantiles of the standardized HCoV-OC43 residuals against the quantiles of a standard normal distribution. D) Residual errors from the HCoV-HKU1 fit on the log scale. E) Q-Q plot of the quantiles of the standardized HCoV-HKU1 residuals against the quantiles of a standard normal distribution. Close alignment between the quantiles of the residuals and the dashed lines in subfigures C and E provide evidence that the residuals are approximately normal-distributed.

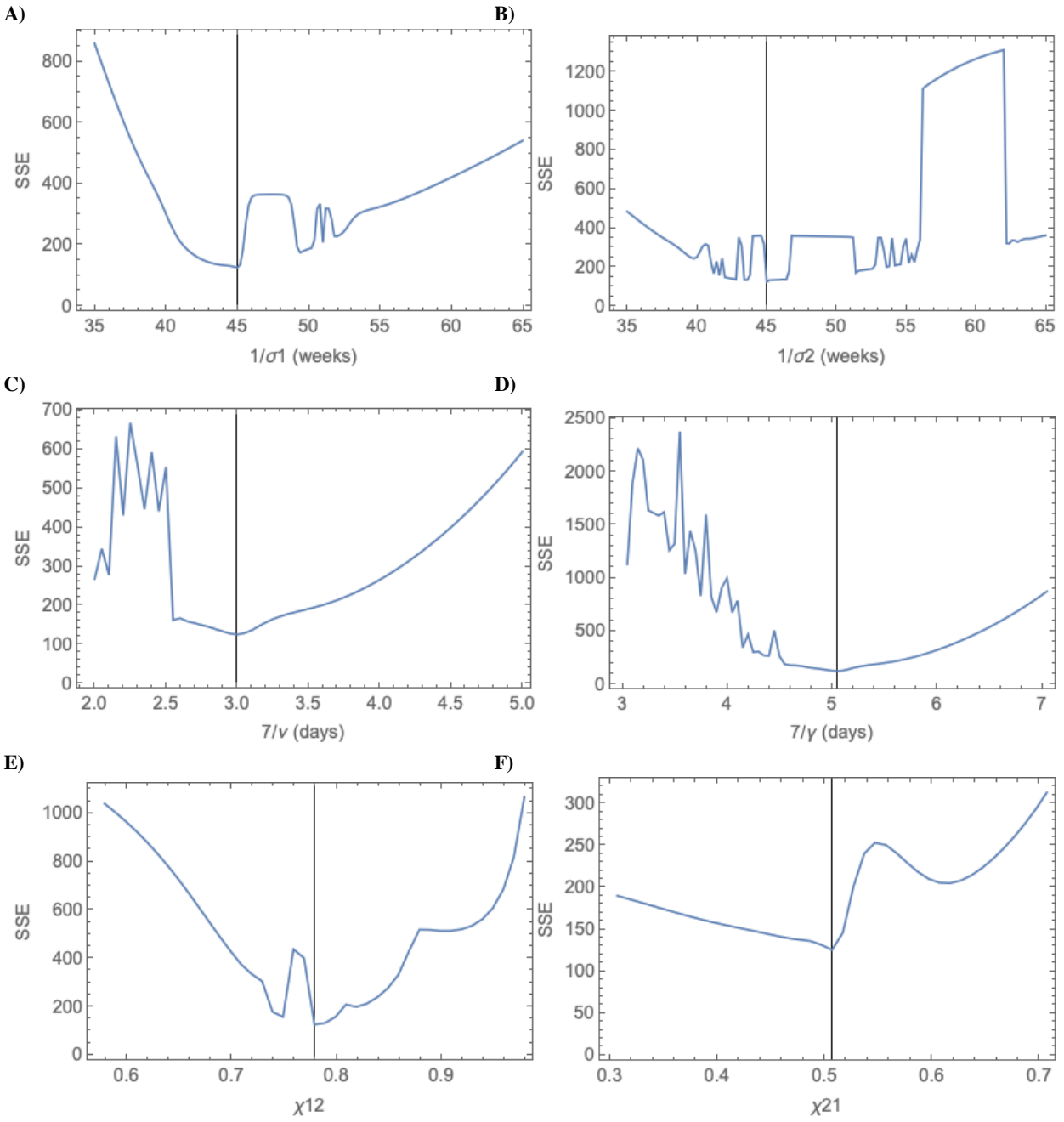
A)
SSE
1/σ1 (weeks)
B)
SSE
1/σ2 (weeks)
C)
SSE
7/v (days)
D)
SSE
7/γ (days)
E)
SSE
χ12
F)
SSE
χ21

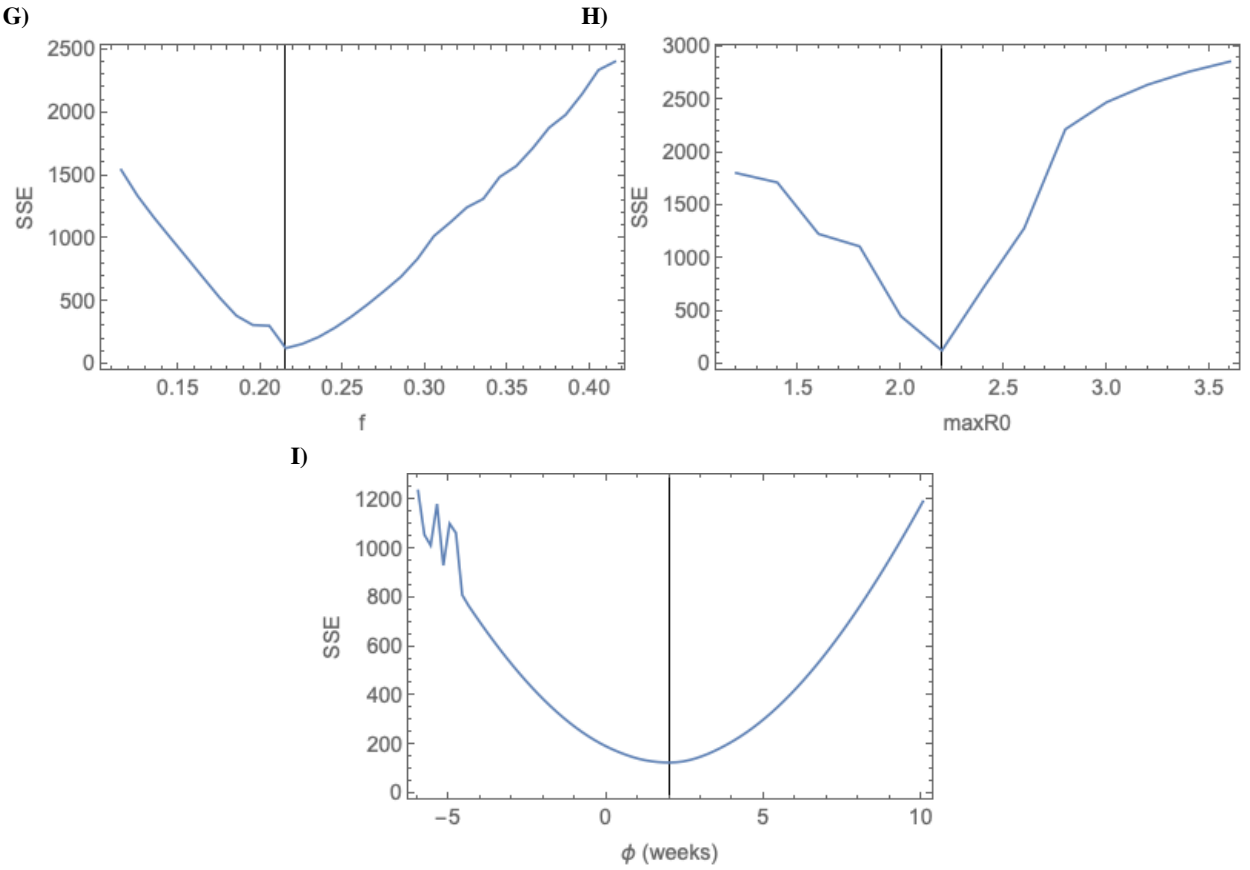

Figure S6. 'Slice' SSE profiles for the parameters of the two-strain SEIRS transmission model. SSE for model parameters (A) σ_1, (B) σ_2, (C) ν, (D) γ, (E) χ_{12}, (F) χ_{21}, (G) f, (H) max(R_0), and (I) ϕ. Each curve is produced by varying the parameter on the horizontal axis while holding the other parameters fixed at their estimated values (**Table S8**). The vertical dashed lines mark the estimated parameter value. Bifurcations in the model solutions lead to a jagged SSE profile, complicating parameter inference. Rather than relying on standard statistical assessments of model fit, we note that the estimated parameter values fall within reasonable epidemiological ranges and provide a good fit to the independently-generated effective reproduction number regression (**Figure 2B-C**).

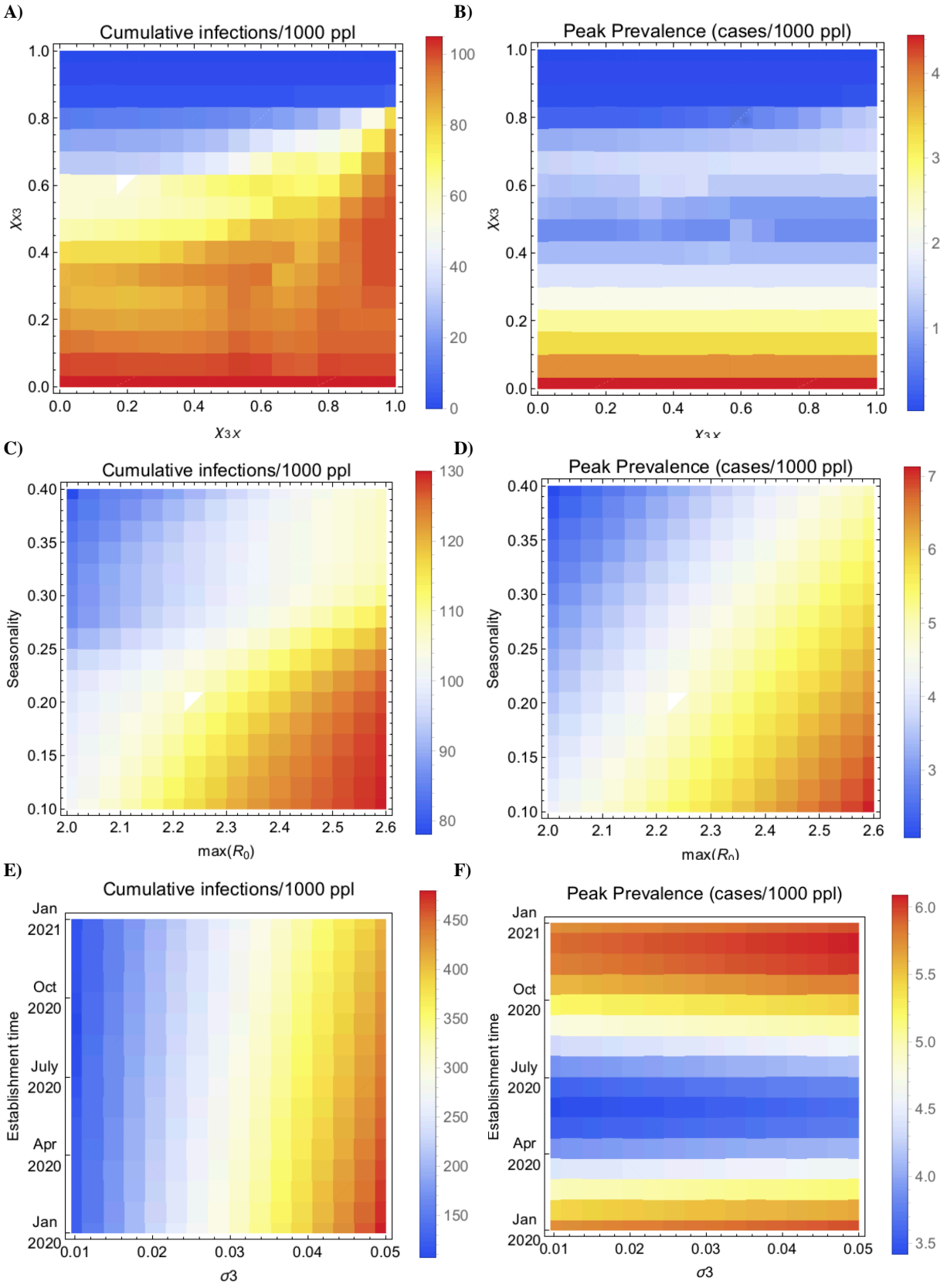
A)
Cumulative infections/1000 ppl
χ_{X3}
χ_{3X}
B)
Peak Prevalence (cases/1000 ppl)
χ_{X3}
χ_{3X}
C)
Cumulative infections/1000 ppl
Seasonality
max(R_0)
D)
Peak Prevalence (cases/1000 ppl)
Seasonality
max(R_0)
E)
Cumulative infections/1000 ppl
Establishment time
Jan 2021
Oct 2020
July 2020
Apr 2020
Jan 2020
σ3
F)
Peak Prevalence (cases/1000 ppl)
Establishment time
Jan 2021
Oct 2020
July 2020
Apr 2020
Jan 2020
σ3

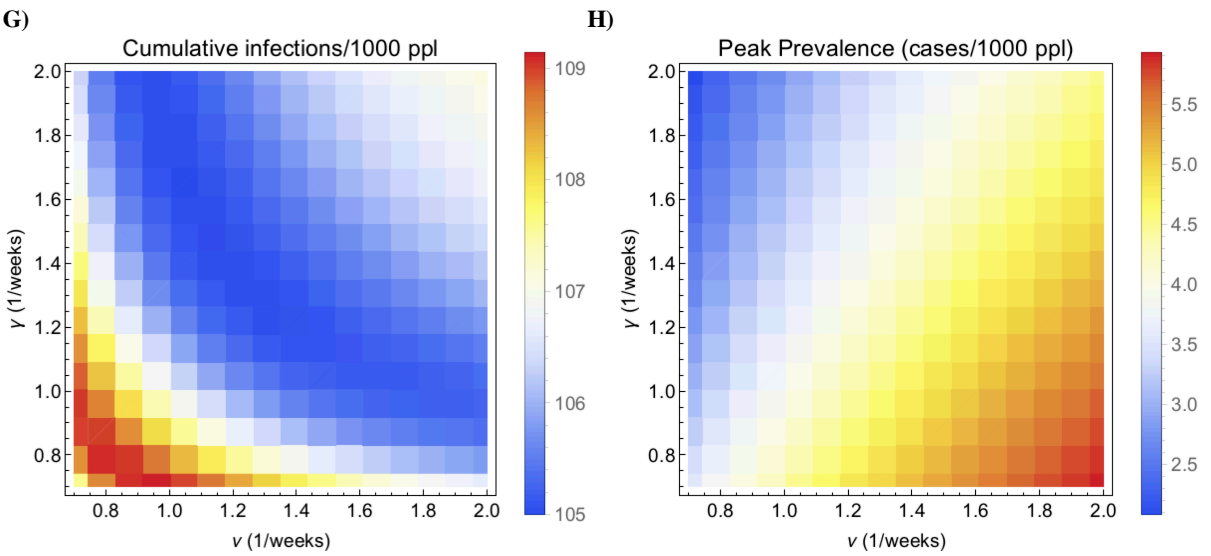

Figure S7. Cumulative infections and peak prevalence for a range of parameter values. Cumulative SARS-CoV-2 infections per 1,000 people (A, C, E) and peak SARS-CoV-2 prevalence per 1,000 people (B, D, F) for (A, B) cross immunities between 0 and 1, (C, D) wintertime R_0 between 2 and 2.6 and seasonality factor f between 10% and 40%, (E, F) $1/\sigma_3$ between 20 and 104 weeks and establishment time between 1 Jan 2020 and 31 Dec 2020, and (G,H) $1/\nu$ and $1/\gamma$ between 3.5 days and 10 days. For each heat map, all parameters other than the two being varied are held constant at their estimated values (**Table S8**) and establishment is on 11 March 2020. High cross immunity from HCoVs OC43/HKU1 against SARS-CoV-2 would lead to fewer cumulative SARS-CoV-2 infections (A) and a lower peak SARS-CoV-2 prevalence (B). Intermediate cross immunity from HCoVs OC43/HKU1 against SARS-CoV-2 leads to high peak prevalence (B) because cross immunity is high enough to push the SARS-CoV-2 peak to the winter, but not high enough to suppress SARS-CoV-2 infection altogether. High R_0 and low seasonality are both associated with higher cumulative SARS-CoV-2 infections (C) and higher peak SARS-CoV-2 prevalence (D). Quickly-waning immunity (σ_3) is strongly associated with high cumulative SARS-CoV-2 infections (E), while autumn/winter establishment is strongly associated with high peak SARS-CoV-2 prevalence (F). Long incubation and infectious periods are associated with a high cumulative number of infections (G), while epidemic peak size is maximized for short latent periods and long infectious periods (H).

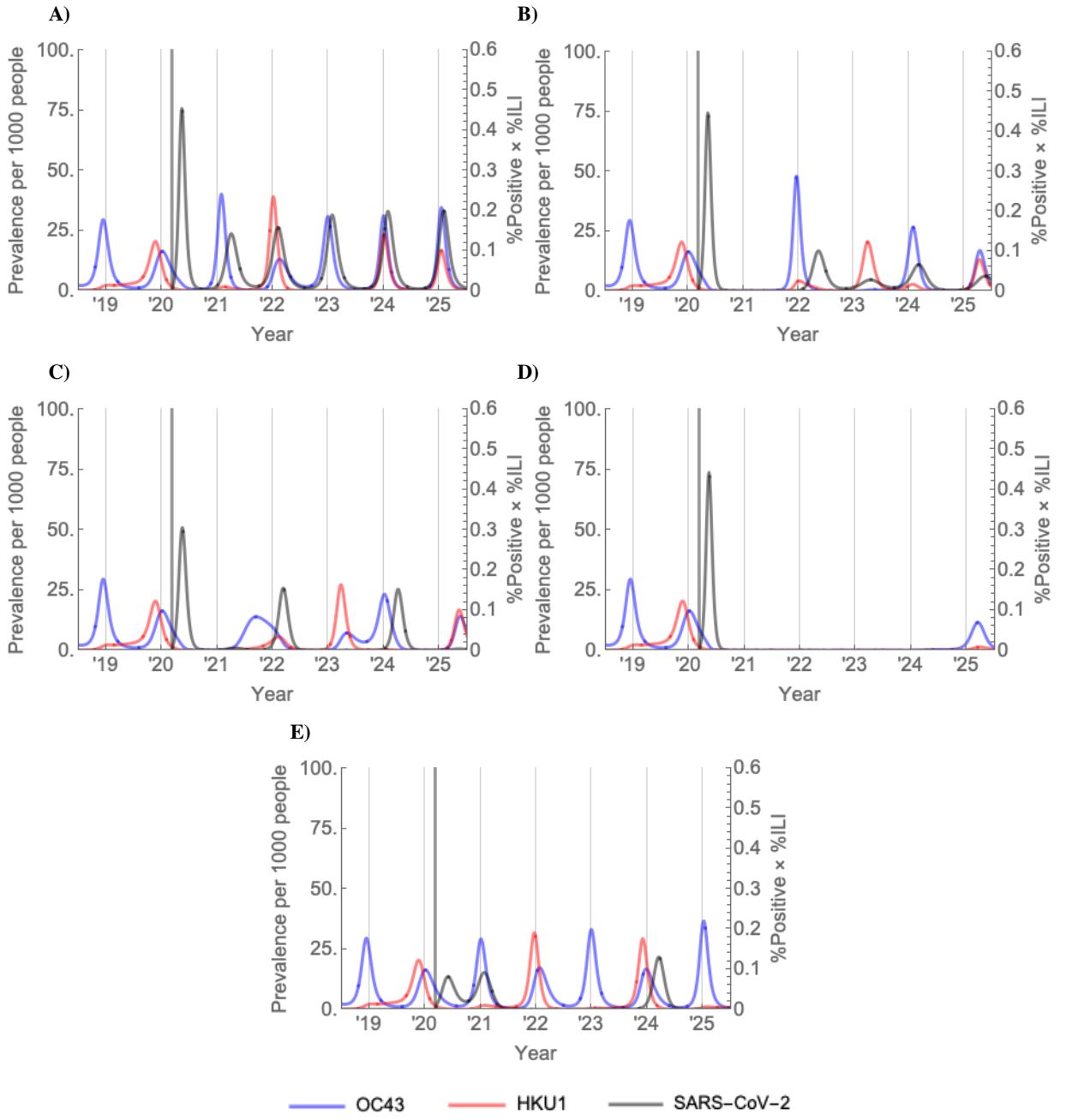

Figure S8. Invasion scenarios for SARS-CoV-2 in temperate regions with max(R_0) = 2.6. These plots depict the prevalence of SARS-CoV-2 (black, cases per 1,000 people), HCoV-OC43 (blue, % positive multiplied by % ILI), and HCoV-HKU1 (orange, % positive multiplied by % ILI) for a representative set of possible pandemic and post-pandemic scenarios using an elevated maximum wintertime R_0 of 2.6. The scenarios were obtained by varying the cross immunity between SARS-CoV-2 and HCoVs OC43/HKU1 (χ_{3X}) and vice-versa (χ_{X3}), the duration of SARS-CoV-2 immunity ($1/\sigma_3$), and the seasonal variation in R_0 (f), assuming an epidemic establishment time of 11 March 2020 (depicted as a vertical grey bar). Parameter values used to generate each plot are listed below; all other parameters were held at the values listed in **Table S8**. (A) A short duration ($1/\sigma_3$ = 40 weeks) of SARS-CoV-2 immunity could yield annual SARS-CoV-2 outbreaks. (B) Longer-term SARS-CoV-2 immunity ($1/\sigma_3$ = 104 weeks) could yield biennial outbreaks, possibly with smaller outbreaks in the intervening years. (C) Higher seasonal variation in transmission (f = 0.4) would reduce the peak size of the invasion wave, but could lead to more severe wintertime outbreaks thereafter (compare with (B)). (D) Long-term immunity ($1/\sigma_3$ = infinity) to SARS-CoV-2 could lead to elimination of the virus. (E) However, a resurgence of SARS-CoV-2 could occur as late as 2024 after a period of apparent elimination if the

duration of immunity is intermediate ($1/\sigma_3$ = 104 weeks) and if HCoVs OC43/HKU1 impart intermediate cross immunity against SARS-CoV-2 (χ_{3X} = 0.3).

(A) $\chi_{3X} = 0.3, \chi_{X3} = 0, 1/\sigma_3 = 40$ weeks, $f = 0.2$
(B) $\chi_{3X} = 0.7, \chi_{X3} = 0, 1/\sigma_3 = 104$ weeks, $f = 0.2$
(C) $\chi_{3X} = 0.7, \chi_{X3} = 0, 1/\sigma_3 = 104$ weeks, $f = 0.4$
(D) $\chi_{3X} = 0.7, \chi_{X3} = 0, 1/\sigma_3 =$ infinity, $f = 0.2$
(E) $\chi_{3X} = 0.3, \chi_{X3} = 0.3, 1/\sigma_3 = 104$ weeks, $f = 0.4$

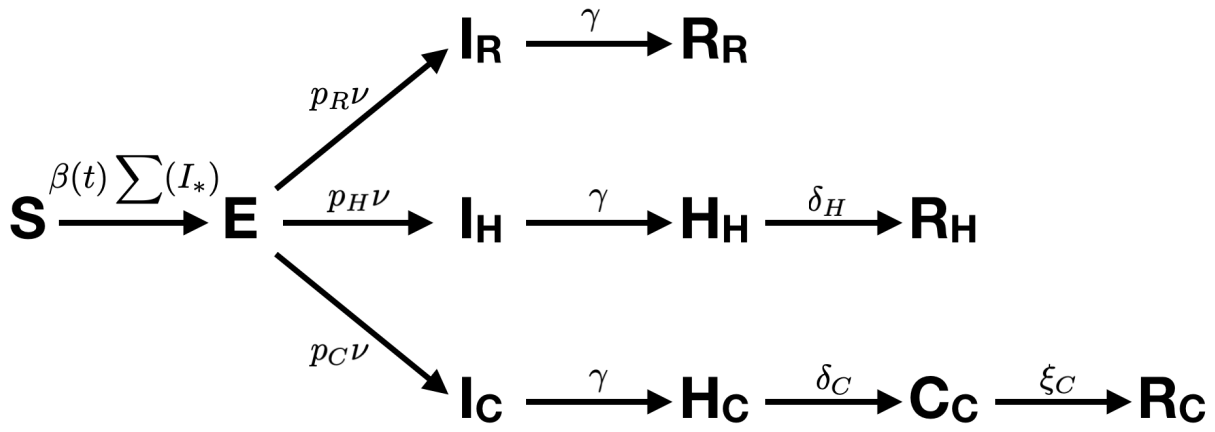

Figure S9. Schematic diagram of the SARS-CoV-2 transmission model accounting for hospitalizations and critical care. The population begins as susceptible (S). Infection is introduced through a half-week pulse in the force of infection of 0.01/week starting on 11 Mar 2020. The transmission rate $\beta(t)$ is a cosine with 52-week period parametrized by a phase shift (ϕ), a maximum value (max(R_0)), and a seasonal forcing factor (f), with values given in **Table S8**. Infected individuals then proceed to an exposed (E) state, after which a proportion $p_R = 0.956$ enters the 'recovery' arm, $p_H = 0.0308$ enters the 'hospitalization' arm, and $p_C = 0.0132$ enters the 'critical care' arm. Exposed individuals become infectious (I) at rate $\nu = 1/4.6$ days. Individuals in the recovery arm then recover (R) at rate $\gamma = 1/5$ days, but individuals in the hospitalization arm must pass through the hospitalization state (H) and individuals in the critical care arm must pass through both the hospitalization (H) and critical care (C) states. The average duration of hospitalization was $1/d_H = 8$ days in the hospitalization arm and $1/d_C = 6$ days in the critical care arm (*26*). The average duration of critical care was $1/\xi_C = 10$ days (*26*).

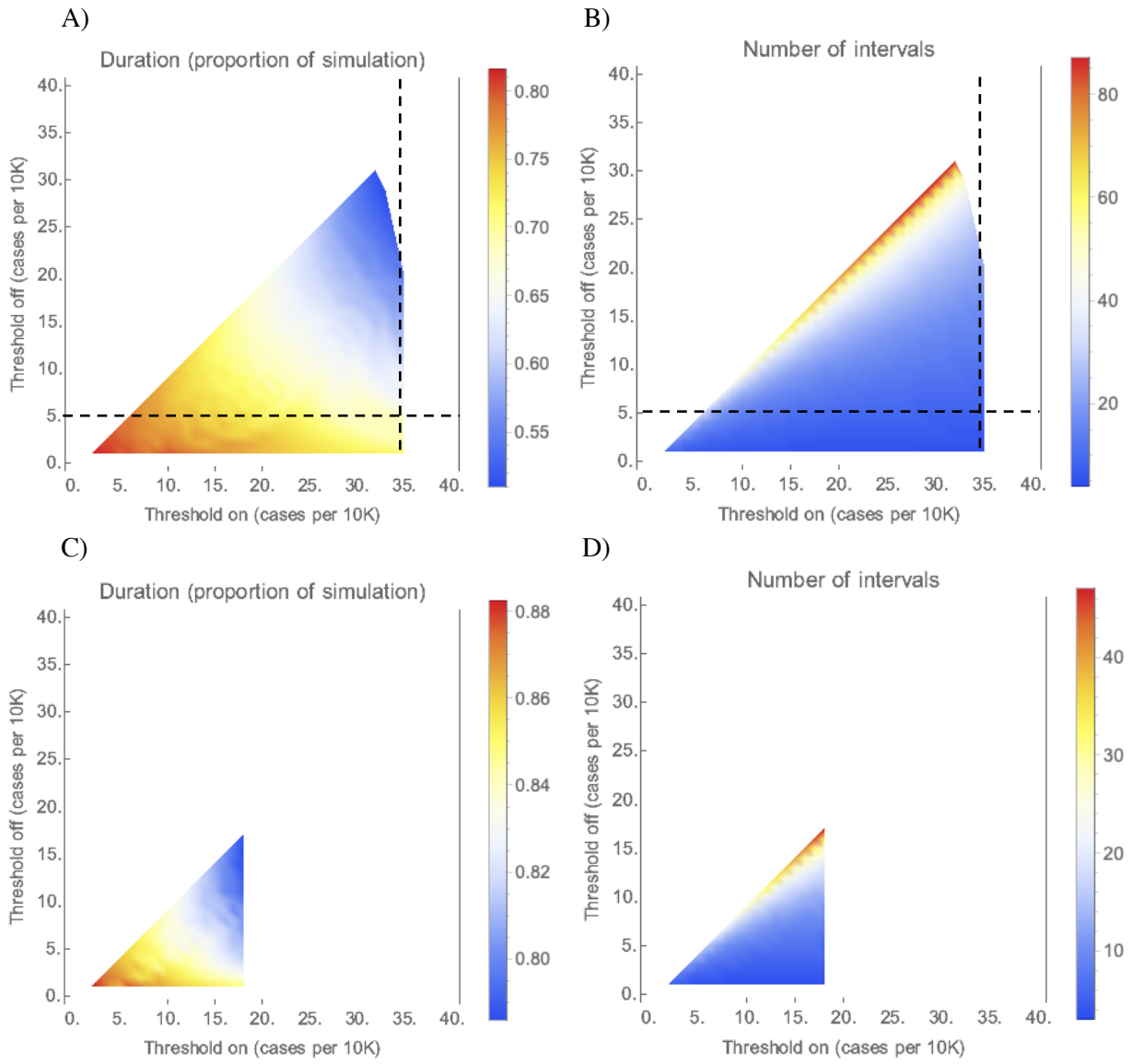

Figure S10. Duration and number of intermittent social distancing interventions through July 2022 as a function of 'on' and 'off' prevalence thresholds, with no seasonality. Duration (A, C) and number (B, D) of social distancing intervals for 'on' and 'off' thresholds between 1 and 40 cases per 10,000 people from simulations with no seasonal variation in transmission. Simulations were run from 1 Jan 2020 through 1 July 2022, with an epidemic establishment time on 11 March 2020. For sub-figures A and B, R_0 is 2.2. For sub-figures C and D, R_0 is 2.6 (note the difference in color scales). The 'on' threshold must be greater than the 'off' threshold (leaving the top-left region of each plot blank) and the number of critical care cases cannot exceed the current US capacity of 0.89 per 10,000 people (leaving the right-hand region of each plot blank). The dashed lines in sub-figures A and B mark the threshold values used to produce **Figure 6A.**

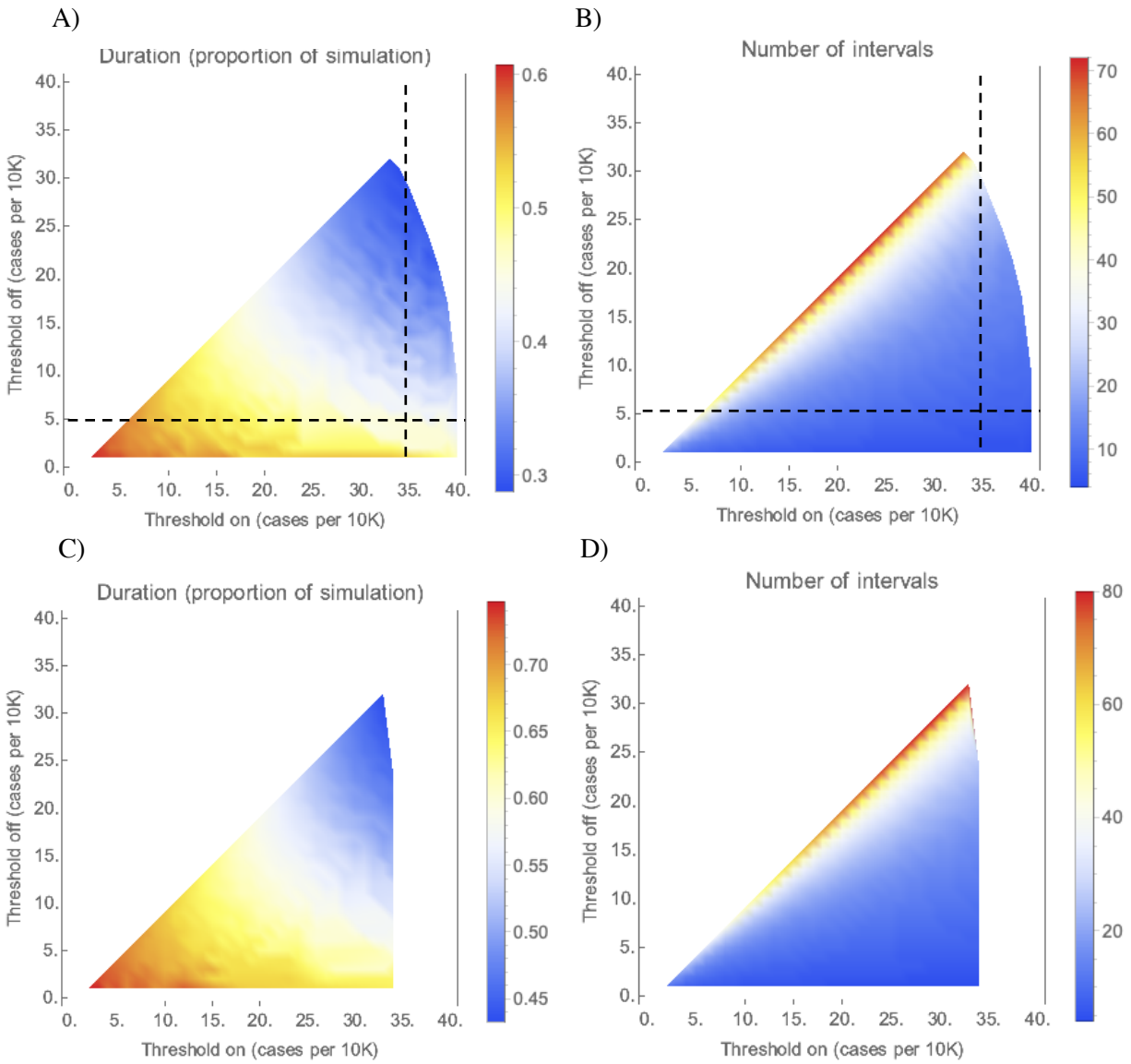

Figure S11. Duration and number of intermittent social distancing interventions through July 2022 as a function of 'on' and 'off' prevalence thresholds, with seasonality. Duration (A, C) and number (B, D) of social distancing intervals for 'on' and 'off' thresholds between 1 and 40 cases per 10,000 people from simulations with seasonal transmission. Simulations were run from 1 Jan 2020 through 1 July 2022, with an epidemic establishment time on 11 March 2020. For sub-figures A and B, the wintertime R_0 is 2.2 and the summertime R_0 is 1.3 (f = 40%). For sub-figures C and D, the seasonality factor is f = 0.4 such that the wintertime R_0 is 2.6 and the summertime R_0 is 1.6 (note the difference in color scales). The 'on' threshold must be greater than the 'off' threshold (leaving the top-left region of each plot blank) and the number of critical care cases cannot exceed the current US capacity of 0.89 per 10,000 people (leaving the right-hand region of each plot blank). The dashed lines in sub-figures A and B mark the threshold values used to produce **Figure 6B.**

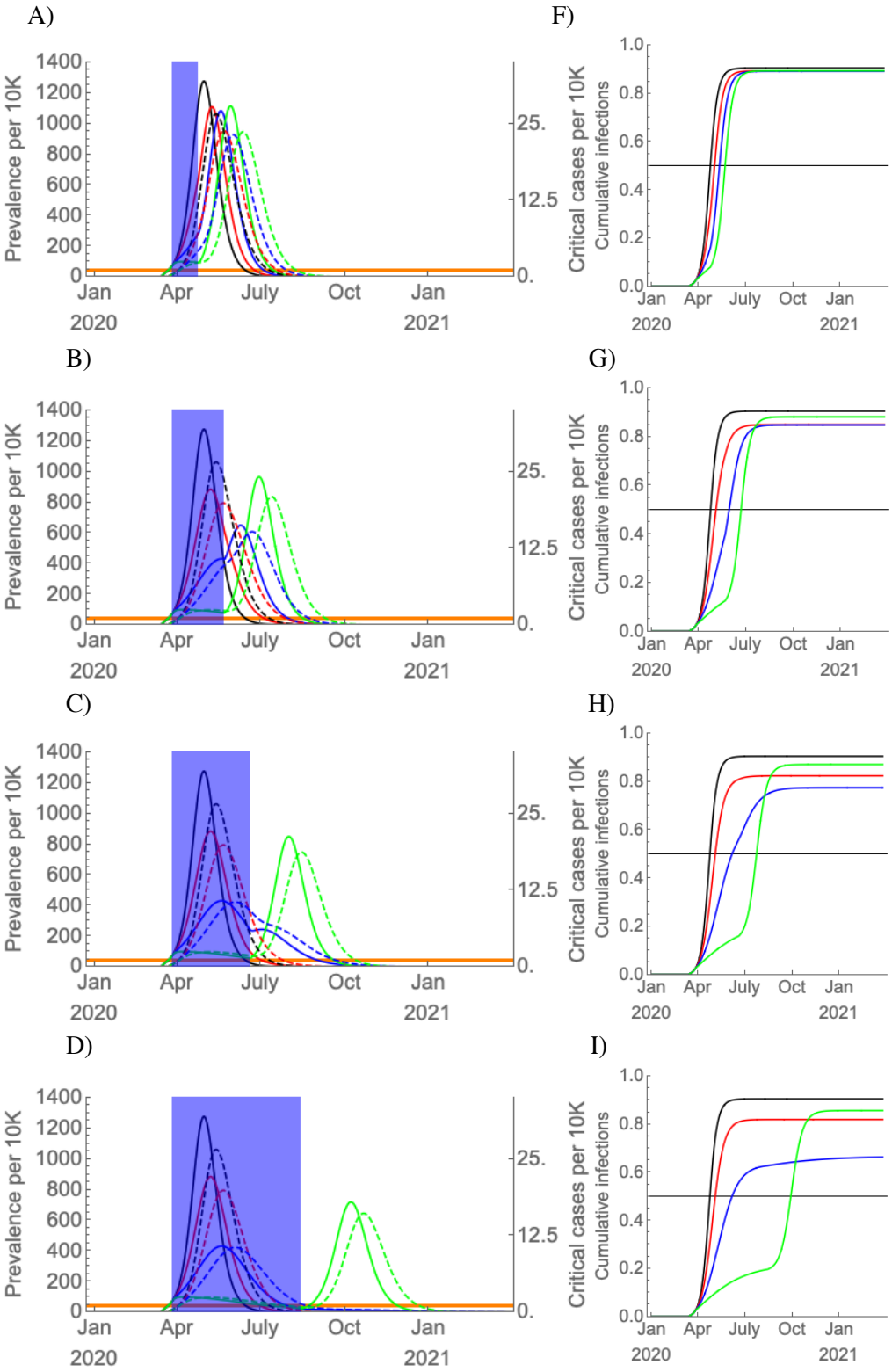
A)
F)
B)
G)
C)
H)
D)
I)
Prevalence per 10K
Critical cases per 10K
Cumulative infections
1400
1200
1000
800
600
400
200
0
25.
12.5
0.
1.0
0.8
0.6
0.4
0.2
0.0
Jan
Apr
July
Oct
Jan
2020
2021

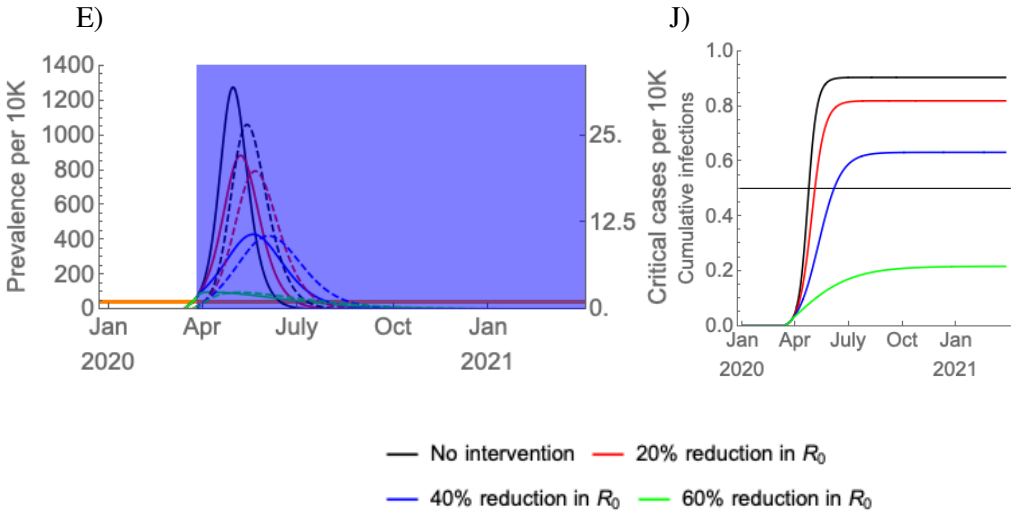

Figure S12. One-time social distancing scenarios in the absence of seasonality with R_0 = 2.6. (A-E) Simulated prevalence of COVID-19 infections (solid) and critical COVID-19 cases (dashed) following establishment on 11 March 2020 with a period of social distancing (shaded blue region) instated two weeks later, with the duration of social distancing lasting (A) four weeks, (B) eight weeks, (C) twelve weeks, (D) twenty weeks, and (E) indefinitely. There is no seasonal forcing; R_0 was held constant at 2.6. The effectiveness of social distancing varied from none to a 60% reduction in R_0. Cumulative infection sizes are depicted beside each prevalence plot (F-J) with the herd immunity threshold (horizontal black bar).

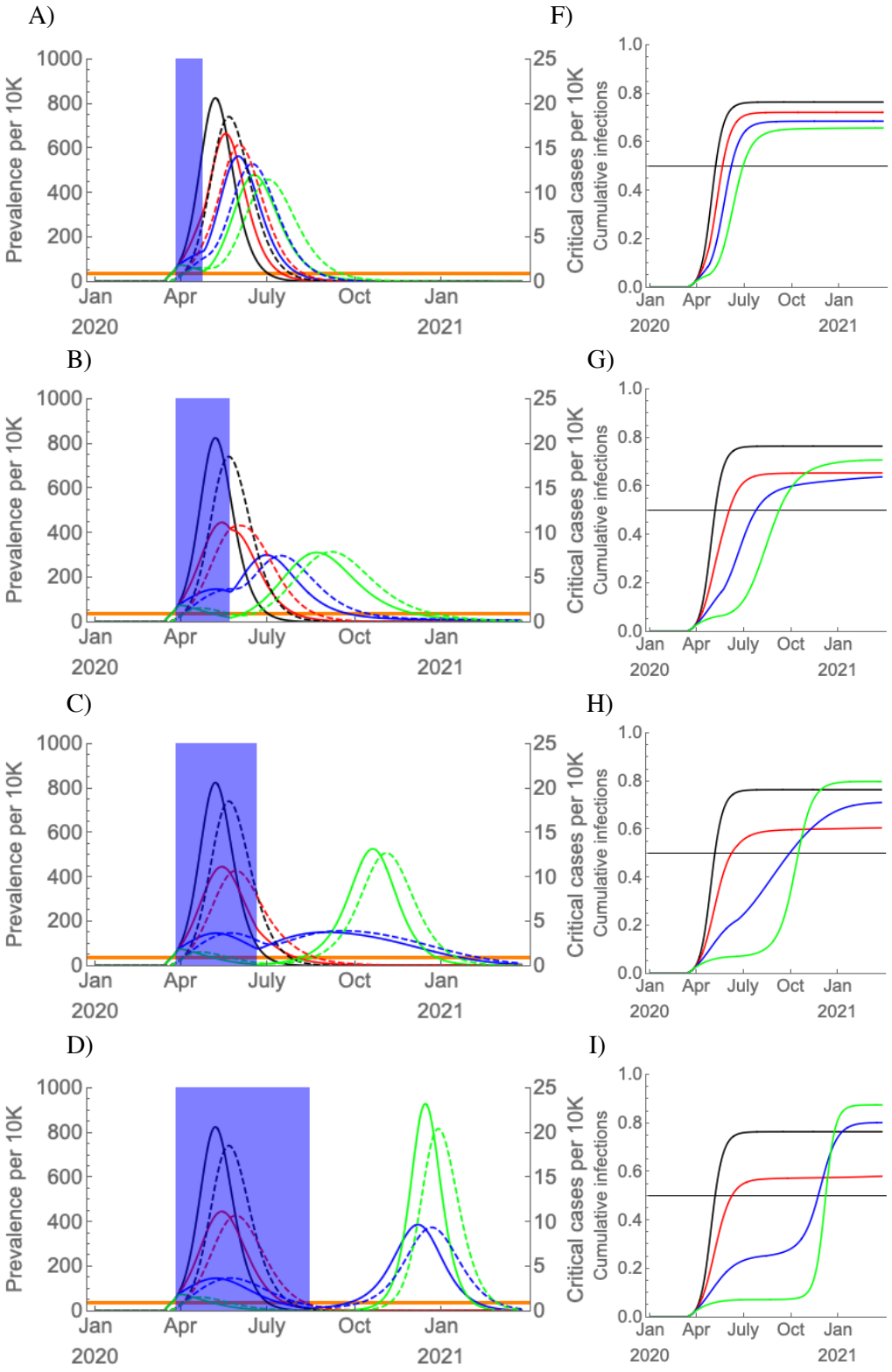
A)
F)
B)
G)
C)
H)
D)
I)
Prevalence per 10K
Critical cases per 10K
Cumulative infections
Jan
Apr
July
Oct
Jan
2020
2021

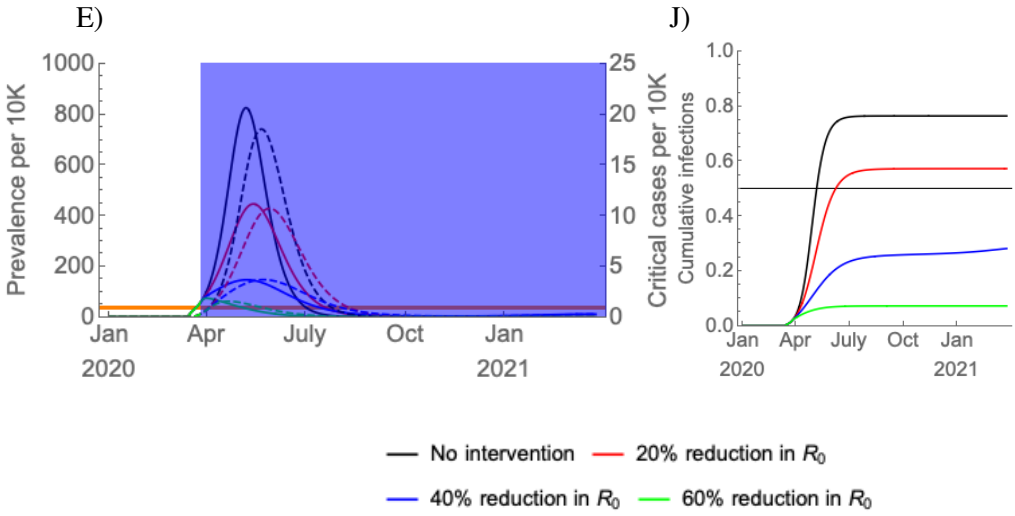

Figure S13. One-time social distancing scenarios with seasonality with R_0 = 2.6. (A-E) Simulated prevalence, assuming strong seasonal forcing (f = 0.4 such that wintertime R_0 = 2.6 and summertime R_0 = 1.6), of COVID-19 infections (solid) and critical COVID-19 cases (dashed) following establishment on 11 March 2020 with a period of social distancing (shaded blue region) instated two weeks later, with the duration of social distancing lasting (A) four weeks, (B) eight weeks, (C) twelve weeks, (D) twenty weeks, and (E) indefinitely. The effectiveness of social distancing varied from none to a 60% reduction in R_0. Cumulative infection sizes are depicted beside each prevalence plot (F-J) with the herd immunity threshold (horizontal black bar). Preventing widespread infection during the summer can flatten and prolong the epidemic but can also lead to a high density of susceptible individuals who could become infected in an intense autumn wave.

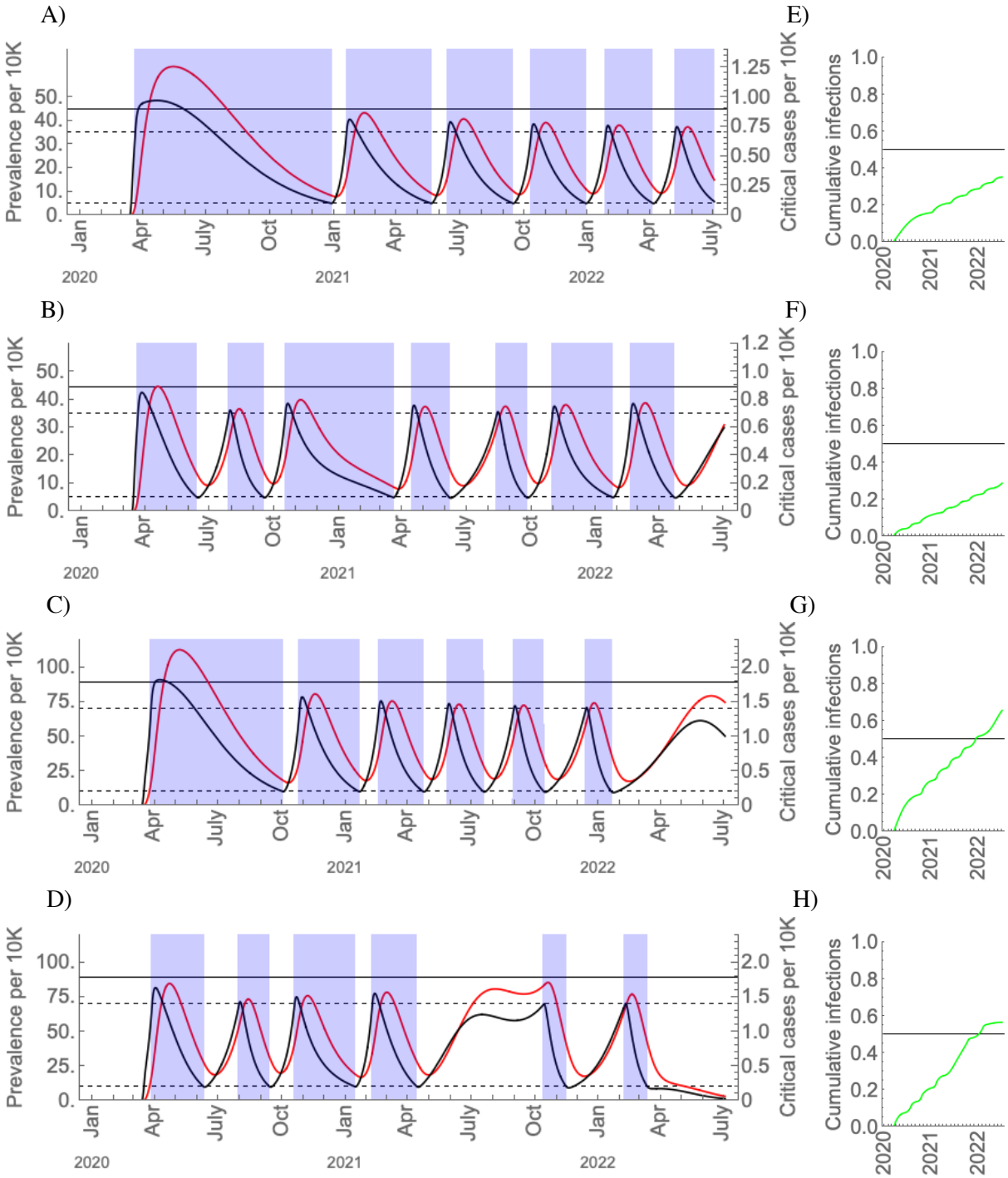

Figure S14. Intermittent social distancing scenarios with current and expanded critical care capacity with R_0 = 2.6. Intermittent social distancing (shaded blue regions) without seasonal forcing (A, C) and with seasonal forcing (B, D) with current critical care capacity (A, B; solid black bar) and double the current critical care capacity (C, D; solid black bar). The on/off thresholds for social distancing are depicted by the dashed horizontal lines. The maximal wintertime R_0 is 2.6 and for the seasonal scenarios the summertime R_0 is 1.6 (f = 0.4). Distancing yields a 60% reduction in R_0. Prevalence is in black and critical care cases are in red. To the right of each main plot (E-H), the proportion immune over time is depicted in green with the herd immunity threshold (horizontal black bar). In the scenarios with no seasonality (B and D), the thresholds critical care capacity is exceeded if the same thresholds are used to trigger the interventions as in the scenario with R_0 = 2.2; in this event, the thresholds

would need to be revised to maintain control of the epidemic. See **Figs S10-11** for a depiction of effective thresholds for $R_0 = 2.2$ and $R_0 = 2.6$, with and without seasonal forcing.

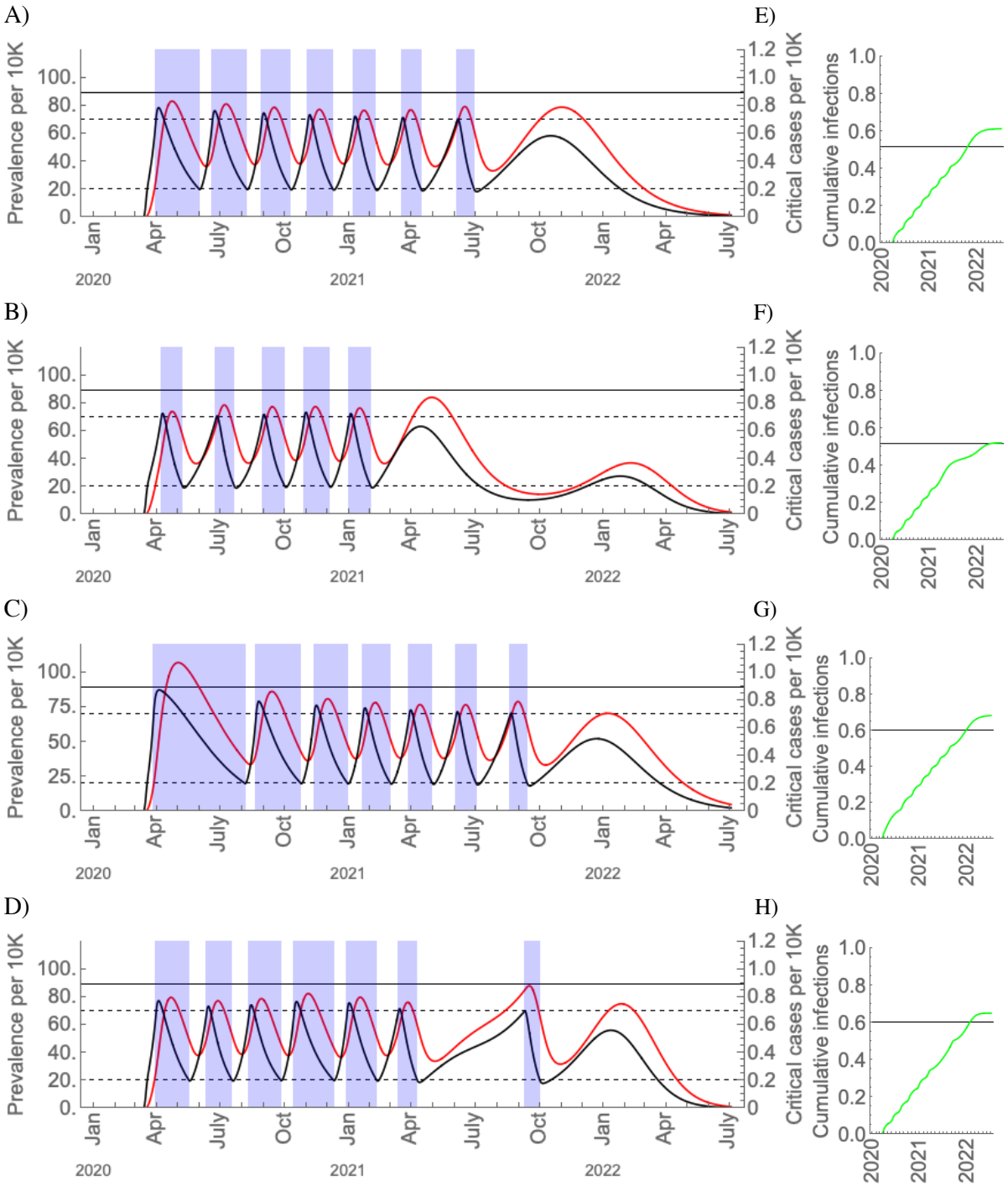

Figure S15. Intermittent social distancing scenarios with a treatment that halves the proportion of infections that are hospitalized. Intermittent social distancing (shaded blue regions) without seasonal forcing (A, C) and with strong seasonal forcing (f = 0.4, B, D) with current critical care capacity and a treatment that halves the probability of needing hospitalization given infection (both p_H and p_C, such that the probability of mild/asymptomatic infection is $p_R + 0.5*p_H + 0.5*p_C$). The on/off thresholds for social distancing are depicted by the dashed horizontal lines. For (A) and (B), the maximal wintertime R_0 is 2.2, while for (C) and (D) the maximum wintertime R_0 is 2.6. Distancing yields a 60% reduction in R_0. Prevalence is in black and critical care cases are in red. To the right of each main plot (E-H), the proportion immune over time is depicted in green with the herd immunity threshold (horizontal black bar). The treatment has a similar effect as doubling critical care capacity.

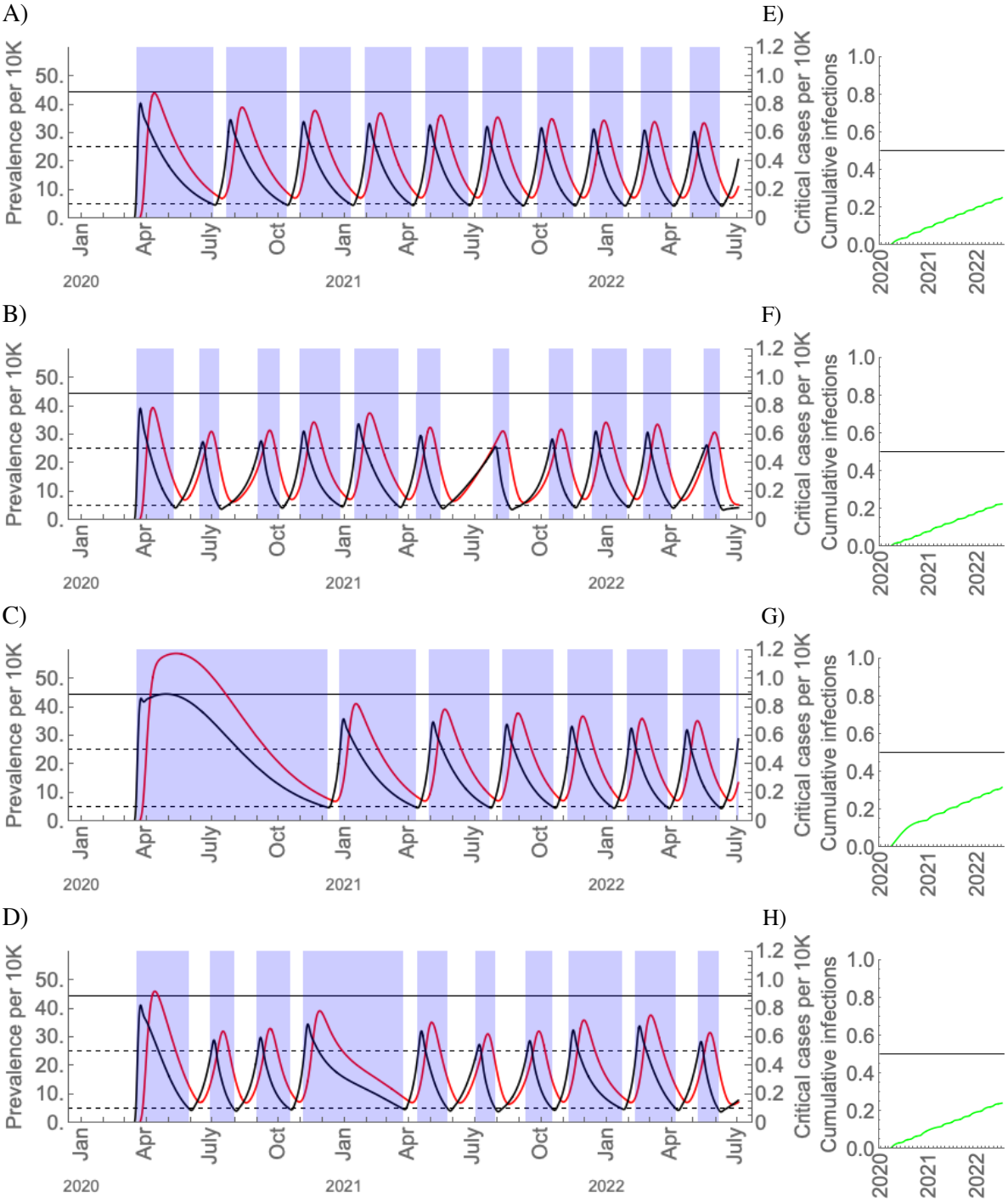

Figure S16. Intermittent social distancing scenarios with gamma-distributed waiting times. Intermittent social distancing (shaded blue regions) without seasonal forcing (A, C) and with strong seasonal forcing (f = 0.4, B, D) with gamma-distributed latent period, infectious period, hospitalization period, and critical care period (see **Figure S17**). The on/off thresholds for social distancing are depicted by the dashed horizontal lines. For (A) and (B), the maximal wintertime R_0 is 2.2, while for (C) and (D) the maximum wintertime R_0 is 2.6. Distancing yields a 60% reduction in R_0. Prevalence is in black and critical care cases are in red. To the right of each main plot (E-H), the proportion immune over time is depicted in green with the herd immunity threshold (horizontal black bar). Compared to the model with exponentially-distributed waiting times, incidence rises more sharply when the waiting times are gamma-distributed, requiring a lower threshold to trigger interventions and leading to more frequent interventions.

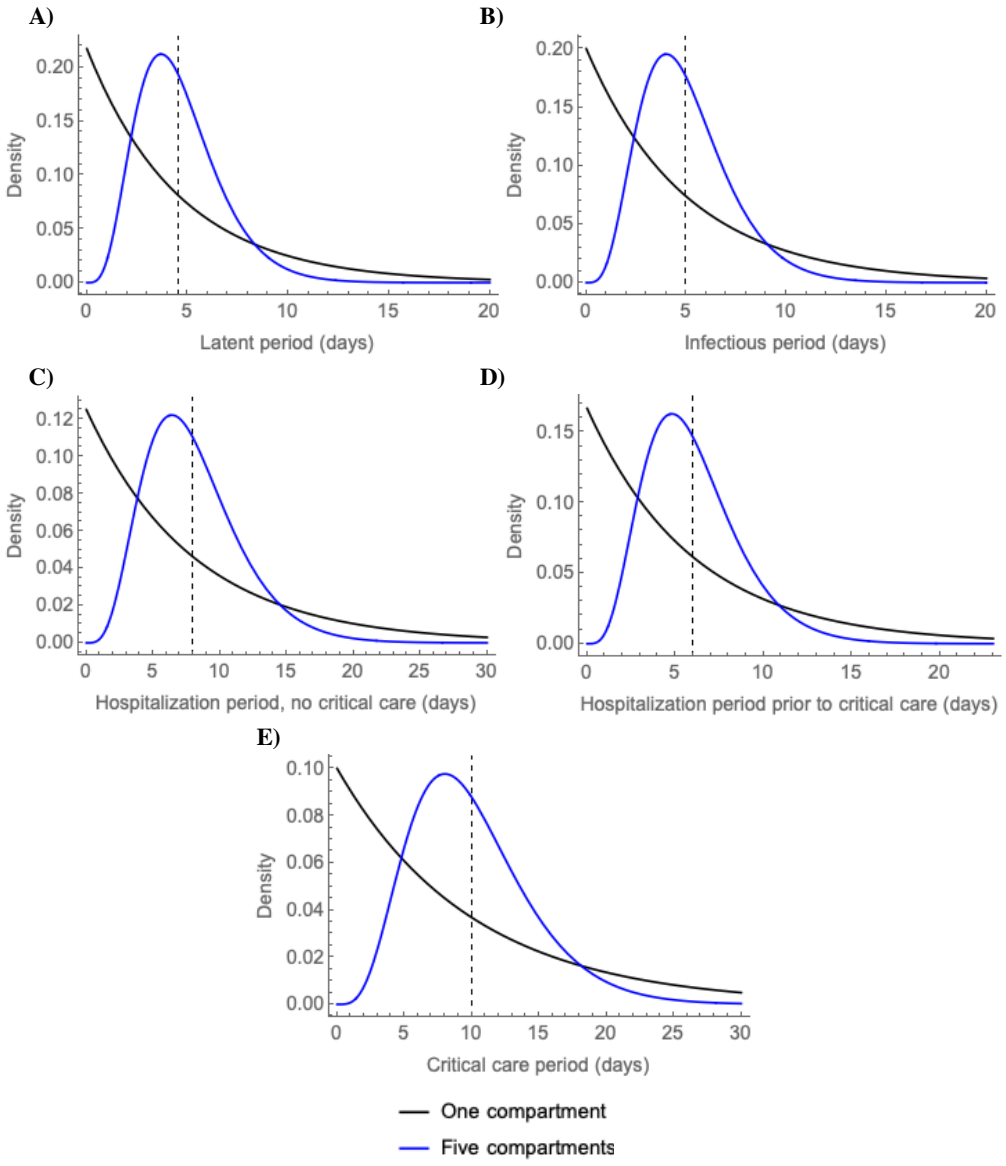

Figure S17. Comparison of exponential and gamma-distributed waiting times for the intervention model. A) latent period (mean 4.6 days); B) infectious period (mean 5 days); C) Hospitalization period without critical care (mean 8 days); D) Hospitalization period followed by critical care (mean 6 days); E) Critical care period (mean 10 days). The exponentially-distributed waiting times are depicted in black and the gamma-distributed waiting times, generated by introducing five 'dummy' compartments for each state, are depicted in blue. The means of the distributions are depicted by the dashed vertical line.

References and Notes

1. World Health Organization, *Coronavirus Disease 2019 (COVID-19) Situation Report – 66* (WHO, 2020); https://www.who.int/docs/default-source/coronaviruse/situation-reports/20200326-sitrep-66-covid-19.pdf?sfvrsn=9e5b8b48_2.

2. R. Li, C. Rivers, Q. Tan, M. B. Murray, E. Toner, M. Lipsitch, The demand for inpatient and ICU beds for COVID-19 in the US: lessons from Chinese cities. medRxiv 2020.03.09.20033241 [Preprint]. 16 March 2020; https://doi.org/10.1101/2020.03.09.20033241.

3. "'Not a wave, a tsunami.' Italy hospitals at virus limit," *AP NEWS*, 13 March 2020; https://apnews.com/a4497f31bf5dbc1ff263e4263fc9f69e.

4. "COVID-19 infections rise in New York with peak weeks away." *AP NEWS*, 25 March 2020; https://apnews.com/7c7563cb82626a4042797c6aa6da260a.

5. D. L. Heymann, J. S. Mackenzie, M. Peiris, SARS legacy: Outbreak reporting is expected and respected. *Lancet* **381**, 779–781 (2013). doi:10.1016/S0140-6736(13)60185-3 Medline

6. Centers for Disease Control and Prevention, *Transcript for the CDC Telebriefing Update on COVID-19* (CDC, 2020); https://www.cdc.gov/media/releases/2020/t0225-cdc-telebriefing-covid-19.html.

7. P. S. Wikramaratna, M. Sandeman, M. Recker, S. Gupta, The antigenic evolution of influenza: Drift or thrift? *Philos. Trans. R. Soc. B Biol. Sci.* **368**, 20120200 (2013). doi:10.1098/rstb.2012.0200 Medline

8. L. Vijgen, E. Keyaerts, E. Moës, I. Thoelen, E. Wollants, P. Lemey, A.-M. Vandamme, M. Van Ranst, Complete genomic sequence of human coronavirus OC43: Molecular clock analysis suggests a relatively recent zoonotic coronavirus transmission event. *J. Virol.* **79**, 1595–1604 (2005). doi:10.1128/JVI.79.3.1595-1604.2005 Medline

9. S. Su, G. Wong, W. Shi, J. Liu, A. C. K. Lai, J. Zhou, W. Liu, Y. Bi, G. F. Gao, Epidemiology, genetic recombination, and pathogenesis of coronaviruses. *Trends Microbiol.* **24**, 490–502 (2016). doi:10.1016/j.tim.2016.03.003 Medline

10. M. E. Killerby, H. M. Biggs, A. Haynes, R. M. Dahl, D. Mustaquim, S. I. Gerber, J. T. Watson, Human coronavirus circulation in the United States 2014-2017. *J. Clin. Virol.* **101**, 52–56 (2018). doi:10.1016/j.jcv.2018.01.019 Medline

11. R. A. Neher, R. Dyrdak, V. Druelle, E. B. Hodcroft, J. Albert, Potential impact of seasonal forcing on a SARS-CoV-2 pandemic. *Swiss Med. Wkly.* **150**, w20224 (2020). doi:10.4414/smw.2020.20224 Medline

12. J. Shaman, V. E. Pitzer, C. Viboud, B. T. Grenfell, M. Lipsitch, Absolute humidity and the seasonal onset of influenza in the continental United States. *PLOS Biol.* **8**, e1000316 (2010). doi:10.1371/journal.pbio.1000316 Medline

13. J. Shaman, E. Goldstein, M. Lipsitch, Absolute humidity and pandemic versus epidemic influenza. *Am. J. Epidemiol.* **173**, 127–135 (2011). doi:10.1093/aje/kwq347 Medline

14. I. Chattopadhyay, E. Kiciman, J. W. Elliott, J. L. Shaman, A. Rzhetsky, Conjunction of factors triggering waves of seasonal influenza. *eLife* **7**, e30756 (2018).

doi:10.7554/eLife.30756 Medline

15. K. A. Callow, H. F. Parry, M. Sergeant, D. A. Tyrrell, The time course of the immune response to experimental coronavirus infection of man. *Epidemiol. Infect.* **105**, 435–446 (1990). doi:10.1017/S0950268800048019 Medline

16. K.-H. Chan, J. F.-W. Chan, H. Tse, H. Chen, C. C.-Y. Lau, J.-P. Cai, A. K.-L. Tsang, X. Xiao, K. K.-W. To, S. K.-P. Lau, P. C.-Y. Woo, B.-J. Zheng, M. Wang, K.-Y. Yuen, Cross-reactive antibodies in convalescent SARS patients' sera against the emerging novel human coronavirus EMC (2012) by both immunofluorescent and neutralizing antibody tests. *J. Infect.* **67**, 130–140 (2013). doi:10.1016/j.jinf.2013.03.015 Medline

17. D. M. Patrick, M. Petric, D. M. Skowronski, R. Guasparini, T. F. Booth, M. Krajden, P. McGeer, N. Bastien, L. Gustafson, J. Dubord, D. Macdonald, S. T. David, L. F. Srour, R. Parker, A. Andonov, J. Isaac-Renton, N. Loewen, G. McNabb, A. McNabb, S.-H. Goh, S. Henwick, C. Astell, J. P. Guo, M. Drebot, R. Tellier, F. Plummer, R. C. Brunham, An outbreak of human coronavirus OC43 infection and serological cross-reactivity with SARS coronavirus. *Can. J. Infect. Dis. Med. Microbiol.* **17**, 330–336 (2006). doi:10.1155/2006/152612 Medline

18. Z. Wu, J. M. McGoogan, Characteristics of and important lessons from the coronavirus disease 2019 (COVID-19) outbreak in China: Summary of a report of 72 314 cases from the Chinese Center for Disease Control and Prevention. *JAMA* **323**, 1239 (2020). doi:10.1001/jama.2020.2648 Medline

19. A. Hauser, M. J. Counotte, C. C. Margossian, G. Konstantinoudis, N. Low, C. L. Althaus, J. Riou, Estimation of SARS-CoV-2 mortality during the early stages of an epidemic: a modelling study in Hubei, China and northern Italy. medRxiv 2020.03.04.20031104 [Preprint]. 6 March 2020; https://doi.org/10.1101/2020.03.04.20031104.

20. R. Verity, L. C. Okell, I. Dorigatti, P. Winskill, C. Whittaker, N. Imai, G. Cuomo-Dannenburg, H. Thompson, P. Walker, H. Fu, A. Dighe, J. Griffin, A. Cori, M. Baguelin, S. Bhatia, A. Boonyasiri, Z. M. Cucunuba, R. Fitzjohn, K. A. M. Gaythorpe, W. Green, A. Hamlet, W. Hinsley, D. Laydon, G. Nedjati-Gilani, S. Riley, S. van-Elsand, E. Volz, H. Wang, Y. Wang, X. Xi, C. Donnelly, A. Ghani, N. Ferguson, Estimates of the severity of COVID-19 disease. medRxiv 2020.03.09.20033357 [Preprint]. 13 March 2020; https://doi.org/10.1101/2020.03.09.20033357.

21. L. Ferretti, C. Wymant, M. Kendall, L. Zhao, A. Nurtay, L. Abeler-Dörner, M. Parker, D. Bonsall, C. Fraser, Quantifying SARS-CoV-2 transmission suggests epidemic control with digital contact tracing. *Science* eabb6936 (2020). doi:10.1126/science.abb6936 Medline

22. R. M. Anderson, H. Heesterbeek, D. Klinkenberg, T. D. Hollingsworth, How will country-based mitigation measures influence the course of the COVID-19 epidemic? *Lancet* **395**, 931–934 (2020). doi:10.1016/S0140-6736(20)30567-5 Medline

23. Q. Bi, Y. Wu, S. Mei, C. Ye, X. Zou, Z. Zhang, X. Liu, L. Wei, S. A. Truelove, T. Zhang, W. Gao, C. Cheng, X. Tang, X. Wu, Y. Wu, B. Sun, S. Huang, Y. Sun, J. Zhang, T. Ma, J. Lessler, T. Feng, Epidemiology and Transmission of COVID-19 in Shenzhen China: Analysis of 391 cases and 1,286 of their close contacts. medRxiv 2020.03.03.20028423 [Preprint]. 27 March 2020; https://doi.org/10.1101/2020.03.03.20028423.

24. N. Thakkar, R. Burstein, H. Hu, P. Selvaraj, D. Klein, Institute for Disease Modeling, Bill & Melinda Gates Foundation, Social distancing and mobility reductions have reduced COVID-19 transmission in King County, WA (Institute for Disease Modeling, 2020); https://covid.idmod.org/data/Social_distancing_mobility_reductions_reduced_COVID_Seattle.pdf.

25. S. Lai, N. W. Ruktanonchai, L. Zhou, O. Prosper, W. Luo, J. R. Floyd, A. Wesolowski, M. Santillana, C. Zhang, X. Du, H. Yu, A. J. Tatem, Effect of non-pharmaceutical interventions for containing the COVID-19 outbreak in China. medRxiv 10.1101/2020.03.03.20029843 [Preprint]. 13 March 2020; https://doi.org/10.1101/2020.03.03.20029843.

26. N. M. Ferguson, D. Laydon, G. Nedjati-Gilani, N. Imai, K. Ainslie, M. Baguelin, S. Bhatia, A. Boonyasiri, Z. Cucunubá, G. Cuomo-Dannenburg, A. Dighe, H. Fu, K. Gaythorpe, H. Thompson, R. Verity, E. Volz, H. Wang, Y. Wang, P. G. Walker, C. Walters, P. Winskill, C. Whittaker, C. A. Donnelly, S. Riley, A. C. Ghani, Impact of non-pharmaceutical interventions (NPIs) to reduce COVID- 19 mortality and healthcare demand (Imperial College COVID-19 Response Team, 2020); https://www.imperial.ac.uk/media/imperial-college/medicine/sph/ide/gida-fellowships/Imperial-College-COVID19-NPI-modelling-16-03-2020.pdf.

27. "Coronavirus: Thousands of extra hospital beds and staff," *BBC News*, 21 March 2020; https://www.bbc.com/news/uk-51989183.

28. C. Chen, B. Zhao, Makeshift hospitals for COVID-19 patients: Where health-care workers and patients need sufficient ventilation for more protection. *J. Hosp. Infect.* S0195-6701(20)30107-9 (2020). doi:10.1016/j.jhin.2020.03.008 Medline

29. "Pentagon says it will give 5 million respirators, 2,000 ventilators to Health and Human Services for virus response," *AP NEWS*, 17 March 2020; https://apnews.com/79e98812b5b1592a134803b00c8d88b0.

30. "Coronavirus: How can China build a hospital so quickly?" *BBC News*, 31 January 2020; https://www.bbc.com/news/world-asia-china-51245156.

31. Centers for Disease Control and Prevention, *The National Respiratory and Enteric Virus Surveillance System (NREVSS)* (CDC, 2020); https://www.cdc.gov/surveillance/nrevss/index.html.

32. E. Goldstein, S. Cobey, S. Takahashi, J. C. Miller, M. Lipsitch, Predicting the epidemic sizes of influenza A/H1N1, A/H3N2, and B: A statistical method. *PLOS Med.* **8**, e1001051 (2011). doi:10.1371/journal.pmed.1001051 Medline

33. Centers for Disease Control and Prevention, *FluView Interactive* (CDC, 2018); https://www.cdc.gov/flu/weekly/fluviewinteractive.htm.

34. J. Wallinga, P. Teunis, Different epidemic curves for severe acute respiratory syndrome reveal similar impacts of control measures. *Am. J. Epidemiol.* **160**, 509–516 (2004). doi:10.1093/aje/kwh255 Medline

35. J. Wallinga, M. Lipsitch, How generation intervals shape the relationship between growth rates and reproductive numbers. *Proc. Biol. Sci.* **274**, 599–604 (2007). doi:10.1098/rspb.2006.3754 Medline

36. D. E. te Beest, M. van Boven, M. Hooiveld, C. van den Dool, J. Wallinga, Driving factors of influenza transmission in the Netherlands. *Am. J. Epidemiol.* **178**, 1469–1477 (2013). doi:10.1093/aje/kwt132 Medline

37. J. M. Read, J. R. Bridgen, D. A. Cummings, A. Ho, C. P. Jewell, Novel coronavirus 2019-nCoV: early estimation of epidemiological parameters and epidemic predictions. medRxiv 10.1101/2020.01.23.20018549 [Preprint]. 28 January 2020; https://doi.org/10.1101/2020.01.23.20018549.

38. S. A. Lauer, K. H. Grantz, Q. Bi, F. K. Jones, Q. Zheng, H. R. Meredith, A. S. Azman, N. G. Reich, J. Lessler, The incubation period of Coronavirus Disease 2019 (COVID-19) from publicly reported confirmed cases: Estimation and application. *Ann. Intern. Med.* (2020). doi:10.7326/M20-0504 Medline

39. N. M. Linton, T. Kobayashi, Y. Yang, K. Hayashi, A. R. Akhmetzhanov, S. M. Jung, B. Yuan, R. Kinoshita, H. Nishiura, Incubation period and other epidemiological characteristics of 2019 novel coronavirus infections with right truncation: A statistical analysis of publicly available case data. *J. Clin. Med.* **9**, 538 (2020). doi:10.3390/jcm9020538 Medline

40. World Health Organization, *Coronavirus Disease 2019 (COVID-19) Situation Report – 51* (WHO, 2020); www.who.int/docs/default-source/coronaviruse/situation-reports/20200311-sitrep-51-covid-19.pdf?sfvrsn=1ba62e57_10.

41. Q. Li, X. Guan, P. Wu, X. Wang, L. Zhou, Y. Tong, R. Ren, K. S. M. Leung, E. H. Y. Lau, J. Y. Wong, X. Xing, N. Xiang, Y. Wu, C. Li, Q. Chen, D. Li, T. Liu, J. Zhao, M. Liu, W. Tu, C. Chen, L. Jin, R. Yang, Q. Wang, S. Zhou, R. Wang, H. Liu, Y. Luo, Y. Liu, G. Shao, H. Li, Z. Tao, Y. Yang, Z. Deng, B. Liu, Z. Ma, Y. Zhang, G. Shi, T. T. Y. Lam, J. T. Wu, G. F. Gao, B. J. Cowling, B. Yang, G. M. Leung, Z. Feng, Early transmission dynamics in Wuhan, China, of novel coronavirus–infected pneumonia. *N. Engl. J. Med.* **382**, 1199–1207 (2020). doi:10.1056/NEJMoa2001316 Medline

42. A. Handel, I. M. Longini Jr., R. Antia, What is the best control strategy for multiple infectious disease outbreaks? *Proc. Biol. Sci.* **274**, 833–837 (2007). doi:10.1098/rspb.2006.0015 Medline

43. C. M. Peak, R. Kahn, Y. H. Grad, L. M. Childs, R. Li, M. Lipsitch, C. O. Buckee, Modeling the comparative impact of individual quarantine vs. active monitoring of contacts for the mitigation of COVID-19. medRxiv 10.1101/2020.03.05.20031088 [Preprint]. 8 March 2020; https://doi.org/10.1101/2020.03.05.20031088.

44. R. J. Hatchett, C. E. Mecher, M. Lipsitch, Public health interventions and epidemic intensity during the 1918 influenza pandemic. *Proc. Natl. Acad. Sci. U.S.A.* **104**, 7582–7587 (2007). doi:10.1073/pnas.0610941104 Medline

45. K. E. Huang, M. Lipsitch, J. Shaman, E. Goldstein, The US 2009 A(H1N1) influenza epidemic: Quantifying the impact of school openings on the reproductive number. *Epidemiology* **25**, 203–206 (2014). doi:10.1097/EDE.0000000000000055 Medline

46. J. Shaman, M. Galanti, Direct measurement of rates of asymptomatic infection and clinical care-seeking for seasonal coronavirus. medRxiv 10.1101/2020.01.30.20019612 [Preprint]. 3 February 2020; https://doi.org/10.1101/2020.01.30.20019612.

47. James Cook University, *State of the Tropics 2017 Report: Sustainable Infrastructure in the Tropics* (James Cook University, 2017); https://www.jcu.edu.au/state-of-the-tropics/publications/2017.

48. D. He, R. Lui, L. Wang, C. K. Tse, L. Yang, L. Stone, Global spatio-temporal patterns of influenza in the post-pandemic era. *Sci. Rep.* **5**, 11013 (2015). doi:10.1038/srep11013 Medline

49. K. S. Vannice, M. C. Cassetti, R. W. Eisinger, J. Hombach, I. Knezevic, H. D. Marston, A. Wilder-Smith, M. Cavaleri, P. R. Krause, Demonstrating vaccine effectiveness during a waning epidemic: A WHO/NIH meeting report on approaches to development and licensure of Zika vaccine candidates. *Vaccine* **37**, 863–868 (2019). doi:10.1016/j.vaccine.2018.12.040 Medline

50. R. Li, S. Pei, B. Chen, Y. Song, T. Zhang, W. Yang, J. Shaman, Substantial undocumented infection facilitates the rapid dissemination of novel coronavirus (SARS-CoV2). *Science* eabb3221 (2020). doi:10.1126/science.abb3221 Medline

51. J. A. Tetro, Is COVID-19 receiving ADE from other coronaviruses? *Microbes Infect.* **22**, 72–73 (2020). doi:10.1016/j.micinf.2020.02.006 Medline

52. Y. Fu, Y. Cheng, Y. Wu, Understanding SARS-CoV-2-mediated inflammatory responses: From mechanisms to potential therapeutic tools. *Virol. Sin.* (2020). doi:10.1007/s12250-020-00207-4 Medline

53. M. U. G. Kraemer, C.-H. Yang, B. Gutierrez, C.-H. Wu, B. Klein, D. M. Pigott, L. du Plessis, N. R. Faria, R. Li, W. P. Hanage, J. S. Brownstein, M. Layan, A. Vespignani, H. Tian, C. Dye, O. G. Pybus, S. V. Scarpino, Open COVID-19 Data Working Group, The effect of human mobility and control measures on the COVID-19 epidemic in China. *Science* **368**, eabb4218 (2020). doi:10.1126/science.abb4218 Medline

54. M. Lipsitch, C. Viboud, Influenza seasonality: Lifting the fog. *Proc. Natl. Acad. Sci. U.S.A.* **106**, 3645–3646 (2009). doi:10.1073/pnas.0900933106 Medline

55. H. V. Fineberg, Ten weeks to crush the curve. *N. Engl. J. Med.* (2020). doi:10.1056/NEJMe2007263 Medline

56. C. Tedijanto, c2-d2/CoV-seasonality: First release, Zenodo (2020); https://zenodo.org/record/3726085#.XpC68_7twwk.

57. S. Kissler, nCoV_introduction, Version 4.0, Zenodo (2020); https://zenodo.org/record/3745557#.XpC7Y_7twwk.

58. M. Lipsitch, T. Cohen, B. Cooper, J. M. Robins, S. Ma, L. James, G. Gopalakrishna, S. K. Chew, C. C. Tan, M. H. Samore, D. Fisman, M. Murray, Transmission dynamics and control of severe acute respiratory syndrome. *Science* **300**, 1966–1970 (2003). doi:10.1126/science.1086616 Medline

59. M. D. McKay, R. J. Beckman, W. J. Conover, Comparison of three methods for selecting values of input variables in the analysis of output from a computer code. *Technometrics* **21**, 239–245 (1979).

60. G. Chowell, C. Viboud, L. Simonsen, S. M. Moghadas, Characterizing the reproduction number of epidemics with early subexponential growth dynamics. *J. R. Soc. Interface* **13**,

20160659 (2016). doi:10.1098/rsif.2016.0659 Medline

61. R Core Team, *R: A language and environment for statistical computing* (R Foundation for Statistical Computing, 2019); https://www.R-project.org/.

62. K. Soetaert, T. Petzoldt, R. W. Setzer, Solving differential equations in R: Package deSolve. *J. Stat. Softw.* **33**, 1–25 (2010); https://www.jstatsoft.org/article/view/v033i09.